"Identifying teleconnections and multidecadal variability of East Asian surface temperature during the last millennium in CMIP5 simulations" by Satyaban B. Ratna et al.

We have responded to the referee's comments in blue text below, as well as modifying our manuscript and providing a new supplement containing some additional supporting results.

Replies to anonymous Referee #1

Ratna et al., examined the relationships between AMO/PDO and surface temperature in East Asia (TAS) at multidecadal time scales based on models and reconstructions data, found that external forcing greatly strengthened the relationship between AMO and TAS but weakened relationship between PDO and TAS, and discussed the volcano influences. This is an interesting study on how external forcing influences on teleconnetions between AMO/PDO and TAS. However, I still have some concerns on this study.

Reply: We thank the referee for their time and for their helpful suggestions.

Major concerns:

1) On the reliability of model and reconstruction data. Comparisons between modeled PDO/AMO from (CCSM4, MPI-ESM-P, BCC) with observed PDO/AMO index from HadISST/NCDC ERSST during the period of 1870-2000 should be added to evaluate the reliability of PDO/AMO index from model. There are several PDO/AMO reconstruction (such as, Gray et al., 2004; Shen et al., 2006). Although such PDO/AMO reconstructions are relatively short, the results seem more convincing by adding these records. In addition, there are published and robust Asian summer temperature reconstructions (e.g. Cook et al., 2013, Shi et al., 2015), such reconstruction data should be used. Comparisons among different reconstructions are as important as comparisons among the different models.

Shen, C., W.-C. Wang, W. Gong, and Z. Hao. 2006. A Pacific Decadal Oscillation record since 1470 AD reconstructed from proxy data of summer rainfall over eastern China. Geophysical Research Letters, vol. 33, L03702, 2006.

Gray, S.T., L.J. Graum-lich, J.L. Betancourt, and G.T. Pederson. 2004. A tree-ring based reconstruction of the Atlantic Multidecadal Oscillation since 1567 A.D. Geophysical Research Letters, 31:L12205, doi:10.1029/2004GL019932.

Cook E R , Krusic P J , Kevin J. Anchukaitis et al. Tree-ring reconstructed summer temperature nomalies for temperate East Asia since 800 C.E. Climate Dynamics, 2013, 41(11-12):2957-2972.

Shi F , Ge Q , Yang B , et al. A multi-proxy reconstruction of spatial and temporal variations in Asian summer temperatures over the last millennium. Climatic Change, 2015, 131(4):663-676.

Reply:

Evaluation of model PDO/AMO. We now include a spatial comparison of the models' PDO/AMO signatures with those observed PDO/AMO, using HadISST and ERSST in Figs. 1 and 2 of our revised manuscript.

Analysis of additional, shorter PDO/AMO reconstructions. The primary focus of this study is on the model simulations and the influence of external forcings, and on records of at least 1000-year length. While analysis of additional reconstructions is worth doing, that is more suited to another study examining shorter periods. We would prefer not to dilute our focus by analysis of additional reconstructions that are shorter (and, since our focus is also exclusively on multidecadal timescales and longer, having millennial-length timeseries is beneficial). Concerning the Gray et al. AMO reconstruction, we note the comments of Wang et al. (2017: disclosure, several authors are also authors of the current study): "The reconstruction of Gray et al. is based on a sparse tree-ring network, completely independent of our predictors; it has precise dating control, but its smaller network (only 12 sites) may compromise its representation of AMV if the centres of climate impact of AMV shift through time (also see the discussions in ref. 16)."

Wang J, Yang B, Ljungqvist FC, Luterbacher J, Osborn TJ, Briffa KR and Zorita E (2017) Internal and external forcing of multidecadal Atlantic climate variability over the past 1,200 years. Nature Geoscience 10, 512-517 (doi:10.1038/ngeo2962).

Analysis of individual Asian summer temperature reconstructions. The E Asian temperature reconstruction we used, from Wang et al. (2018), is a composite of seven published reconstructions that already *includes* the two suggested by the referee (Cook et al. 2013, Shi et al. 2015). The time series comparison of these three datasets can be seen in Wang et al (2018). Nevertheless, we have calculated the correlations between three of the individual summer temperature reconstructions (Cook et al. 2013, Shi et al. 2015, Zhang et al. 2018) and AMO (Wang et al. 2017, Mann et al. 2009), PDO (Mann et al. 2009, MacDonald et al. 2005), volcanic (GRA, Gao et al. 2008; CEA, Crowley et al. 2008; SIG, Sigl et al. 2015) and solar forcing (VSK, Vieira et al. 2011; DB, Delaygue and Bard (2011); SBF; Steinhilber et al. 2009). They do show some interesting differences, perhaps related to how well they resolve the response to volcanic forcing, so we have included these additional results in the supplementary material of our revised manuscript (Fig. S3). However, with the exception of the correlations between E Asian temperature and the Mann et al. (2009) AMO index, the only significant correlations (with some solar forcing, PDO and AMO reconstructions) at the multidecadal timescales are with the Wang et al. (2018) composite reconstruction.

2) On PDO signal. PDO has clear decadal and inter-decadal signal. Figure 11 also showed significant 15-20 years periods for PDO. However, all the time series are passed through a 30-year low pass filter using the Lanczos filter, which may miss key information of PDO. 10-year low pass filter should be used for PDO analysis.

Reply: We agree that PDO has a decadal signal which can been identified in Figure 11. However, the

specific purpose of our study is to look at variability on *multidecadal* timescales (title and first line of the abstract), not decadal timescales, which is why we have passed all timeseries (including the PDO) through a 30-year low-pass filter. Therefore we do not use a 10-year filter because that would conflict with the aim of our study.

3) On Volcano influences. Although previous studies showed that volcano eruptions affected decadal climate changes, it is equivocal that volcano eruptions affected multidecadal climate changes. For example, TAS reconstruction showed clear volcanic forcing signal, and volcano eruptions resulting in pulses of cooler summer conditions that may persist for several years (See Figure 12 in Cook et al., 2013). However, this study showed that there were not significant correlations between TAS and volcanic forcing (Figure 8c). In addition, superposed epoch analysis (SEA) should be used to test the impact of explosive volcanism on temperature.

Reply: Again, we note the aim of our study is explicitly to look at *multidecadal* timescales, so a superposed epoch analysis would not add more to the results already found. However, as noted above, we have now also analysed three individual E Asian temperature reconstructions, including Cook et al. (2013). Although the correlations with volcanic forcing are slightly stronger for Cook et al. (2013) than for the other reconstructions (Fig. S3 of our revised manuscript), they are still not statistically significant at the multidecadal timescale. This contrasts with six of the seven climate models, which show significant multidecadal correlations between simulated E Asian T and volcanic forcing, a finding that we report in the paper. There is also evidence that volcanic eruptions affect heat content and SST on these longer timescales (e.g. Gleckler et al. 2006). As suggested by the referee, the volcanic influence on the reconstructed temperatures is probably limited to the interannual timescale – but this timescale is not the focus of our study.

Gleckler, P. J., T. M. L. Wigley, B. D. Santer, J. M. Gregory, K. AchutaRao, and K. E. Taylor, 2006: Volcanoes and climate: Krakatoa's signature persists in the ocean. Nature, 439, 675.

4) On time scales of external forcing. there are other external forcings (e.g. solar activity) that should be considered. Solar activity has multi-decadal periods.

Reply: We focussed on volcanic forcing because it had previously been established that this was the largest external influence on the last millennium simulations (see the first paragraph of section 5 of our manuscript). However, since we are also looking at reconstructions, the referee is correct that we should not neglect solar forcing, because the reconstructions might show a significant association with solar forcing (indeed, as Wang et al. 2018 showed) even though the models may not. We have now included solar forcings in our analysis of the correlations between E Asian temperature and PDO/AMO/external forcing, both in model and reconstructions (Figs. 7 and 8 of our revised manuscript). We used three different solar forcing reconstructions (Vieira et al. 2011; DB, Delaygue and Bard (2011); Steinhilber et

al. 2009). The only E Asian temperature reconstruction with significant multidecadal correlations to solar forcing is the composite reconstruction of Wang et al. (2018).

5) On influences of external forcing, external forcing greatly strengthened the relationship between AMO and TAS but weakened relationship between PDO and TAS. Do you think such results are related to definition and calculation of AMO and PDO? In simple terms, AMO reflects average SST, but PDO reflects spatial configuration of SST. So AMO may be related to external forcing while PDO may be related to internal variability.

Reply: Yes, the referee's explanation is correct.

Minor Concerns:

1) Page 3, Line 20-22. For temperature over East Asia, TAS reconstruction is summer temperature, and TAS model data is summer, cold season temperature and annual temperature. It is confusing. Please clarify which season temperature used in Figure 3-8 in Figure caption.

Reply: The annual mean temperature is used in Figures 3-8. We have amended the figure captions to make this clear.

2) Page 13, Line 9, East Asiantemperature should be East Asian temperature.

Reply: We have corrected this typo.

3) Figure 7a, the label for y axis for volcanic forcing should be added.

Reply: We have added the y-axis label for volcanic forcing: 'Radiative forcing (W m^{-2})'

4) Figure 8, confidence level explanation should be added.

Reply: We have changed the way that we mark the significant correlations (bold symbols or dashed lines for significance levels) and we have added to the captions that these indicated 'values significant at 95% level using a two-tailed student t-test'.

Replies to Anonymous Referee #2

General Comments: Ratna et al. examine the influence of transient external forcing (volcanic eruptions) on PDO and AMO variability and teleconnection patterns as they relate to East Asian surface air temperatures (SAT) in three PMIP3/CMIP5 past1000 simulations and paleoclimate reconstructions. This is an interesting study, and the results have interesting implications for how external forcing can impact internal variability and teleconnections. However, more work is needed to compare model output to observations and expand the study to other models.

Reply: We are grateful to the referee for their careful review and that they consider our work to be of interest. We respond below to the suggestions for expanding the scope of the work.

Main Concerns:

1) There are at least ten CMIP5/PMIP3 past1000 (Last Millennium) simulations available on ESGF that span the 850-1849 CE time period (BCC, CCSM4, CSIRO, FGOALS, GISS, Had, IPSL, MIROC, MPI, MRI). The authors exclude several of these simulations (MIROC, FGOALS, GISS) due to spin up/model drift/trend issues and cite Atwood et al for why they exclude these simulations. However, the authors choose not to use the output from CSIRO, HadCM3, IPSL, or MRI (some of which are included in the analysis of Atwood et al). The results therefore seem incomplete and selectively presented- why the exclusion of these other simulations? Please include analyses of these other Last Millennium simulations or at least provide a reason for why these other Last Millennium simulations have been excluded (the data have been available for at least 8-12 months online, so I hope it's not a data availability issue?). As the manuscript is currently written, 1/3 of the models show a completely different result, but this is only one model- is this really 1/3 of all CMIP5 Last Millennium models, or just one outlier in the CMIP5 Last Millennium simulations?

Reply: We originally considered all six models that had CMIP5/PMIP3 Last Millennium and CMIP5 historical simulations and that had data for all the necessary variables in the UK JASMIN facilities. We then discarded three due to drift issues as explained in our manuscript. Following the referee's recommendation, we sought data for the additional models suggested from other parts of the ESGF and we obtained sufficient data to extend our study to another four CMIP5 models (HadCM3, MRI, IPSL and CSIRO-Mk3L-1-2). We agree that our revised manuscript has been strengthened by including these additional model results. Some of the results are similar, but there are some differences in the correlations with E Asian temperature that we discuss in our revised manuscript.

2) The authors concatenate the Last Millennium (850-1849CE) and the Historical simulations (1850-2005CE) after removing the linear trend from each of these time segments separately. Removing a linear trend from either instrumental or CMIP5 data over the entire 1850-2005CE time period can be problematic if the main component of the 'warming trend' is in the 20th century. Multiple papers choose to remove the linear trend over the 20th century only (e.g., Deser et al., 2010; Messie and Chavez, 2011;

Franzke, 2014, Nature Climate Change; Ji et al., Nature Climate Change, 2014). Similarly, many CMIP5 historical simulations appear to show much of the global warming trend starting in the 20th century, so removing a trend over the full historical simulation period (1850-2005) may add in decadal-centennial variability. To avoid this detrending and concatenation problem, could the analysis just be conducted over the 850-1849CE time period (especially because it seems the authors are mostly focused on the impacts of volcanic eruptions on the PDO and AMO in the pre-1850CE time period?). Some recent work even suggests that the dynamics of the system change once GHG forcing becomes dominant (e.g., Song and Yu, 2015, J Clim; Brown et al., 2017, Nature Climate Change), so including this time period could be arguably problematic.

Reply: We recognise the referee's concerns about linearly detrending the Historical simulations, but our findings are not sensitive to this choice.

We note that we are trying to replicate in the models some aspects of what other studies have done using observations (proxy-based reconstructions and/or instrumental) and (a) in some cases linear detrending over the instrumental era is done even though it may not be optimal for the reasons given by the referee; and (b) the timing of the start of the anthropogenic warming can be in conflict with a linear detrending that begins in 1850 but this would be ameliorated for the PDO and for the AMOrem indices by the prior removal of global-mean SST from the Atlantic or Pacific SST values.

Nevertheless, we have tested to see whether our findings are sensitive to this issue by restricting the analysis to only the Last Millennium simulation and found that our results are quite similar to those we obtained by the combined detrended LM plus detrended historical simulations (compare columns of Figs. S1 and S2 for correlations with E Asia temperature for AMO and PDO, respectively).

We report this sensitivity test in the revised manuscript and discuss the few small differences that do occur. We keep the main results based on the combined LM+Historical analysis because the benefits of having a longer series to analyse outweighs the concerns raised now that we have shown that our findings are not sensitive to this issue.

3) There is no comparison between the spatial patterns of the AMO and PDO in instrumental-based reconstructions and the three models used here- perhaps some of these simulated spatial patterns are more realistic than others? The authors state that the model results are realistic, but never show this in the manuscript. The Climate Variability Diagnostics Package (http://webext.cgd.ucar.edu/Multi-Case/CVDP_ex/CMIP5-Historical/) shows that the spatial expressions of the AMO (and PDO) can be quite different in the various CMIP5 Historical simulations. Interpretation of the model results may be viewed through a more informed perspective if the models are compared to instrumental-based observations.

Reply: We now include a comparison of the AMO and PDO patterns with the instrumental data (similar comment from referee 1) in our revised Fig. 1 and 2.

4) Varying significance levels are used in the paper (90% vs 95%). Please use a consistent 95% or 99% significance level- as the paper stands, it appears that the significance level has been lowered to show 'significance spectral peaks' (e.g., Fig 10), but the spectra barely surpass this 90% level- why not use 95% or 99% everywhere? At least please include some discussion of the sensitivity of the results to significance level if the results don't pass this higher threshold (significance levels are admittedly is arbitrary, but the current, inconsistent use of 90% runs the risk of appearing selectively low to attempt to present a 'significant' result).

Reply: Significance tests are reported for three types of analysis in the manuscript. (1) For correlations between area-averaged temperature and driving factors (bar charts) we used the 'standard' 95% level. (2) For correlations between temperature fields and driving factors (contoured maps) we lowered this to the 90% level because the additional noise at the grid cell level increases the risk of a type II error (wrongly failing to reject the null hypothesis that there is no correlation). (3) For power spectra of AMO and PDO, we used a 90% level, but actually our interest is not really in the significance of the individual spectral peaks (and whether they pass an arbitrary level or not) but in the overall shape of the spectra, their redness and broad multi-decadal power, and whether these are similar between models, with/without forcing, and between AMO index definitions. We explain this better in the revised manuscript and we removed the significance lines from the spectra.

General minor issues:

Many authors abbreviate pre-industrial Control as PI (e.g., Atwood et al., 2016, J Clim, among others)- in an effort to maintain some sort of standard abbreviation that may be quickly recognized, I would encourage the authors to employ more commonly used acronyms (e.g., PI or piControl).

Reply: We modified the manuscript to use the abbreviation PI for pre-industrial Control.

Also, when reading through the figures, it is difficult to interpret the acronyms used in each figure without searching through the other figure captions or the text for the definitions of the acronyms- please define the acronyms used in each figure in each figure caption (or at least reference where they are defined) so readers can quickly understand the figure without searching for what they mean.

Reply: We now define the acronyms in the Figure captions.

Specific comments:

Page 1, Line 12-13: The simulated PDO and AMO spectra and spatial patterns are never compared to instrumental-based patterns or spectra (or even to proxy-based spatial patterns). Please include figures/analysis that support this statement in the main text or remove it.

Reply: We now include a comparison of the AMO and PDO patterns with the instrumental data (Fig. 1 and 2). We have also compared the spectrum of reconstruction and instrumental data for both AMO (Fig. 10) and PDO (Fig. 11).

Page 2, _line 10: The previous paragraph critiques the instrumental and proxy-based records, but little attention is paid to potential model deficiencies- can you at least briefly discuss or cite a few papers that may critique or even acknowledge that CMIP5/PMIP3 models have their own biases and problems as they relate to low-frequency SAT variability (e.g., Laepple and Huybers, 2014; Parsons et al., 2017 J Clim;) or 'modes' of internal variability (or their responses to stratospheric aerosol loading from volcanic eruptions)? Alternatively, directing the reader to where these model deficiencies, and their implications for your results, are going to be discussed later in the paper could be helpful.

Reply: we now cite these references and added a few sentences to describe their implications for potential model deficiencies. We discuss that Laepple and Huybers (2014) found potential deficiencies in CMIP5 SST variability, with model simulations diverging from a multiproxy estimate of SST variability (that is consistent between proxy types and with instrumental estimates) toward longer timescales. Parsons et al. (2017) found very different pictures of natural variability between CMIP5 models, including the North Atlantic, and between models and paleoclimate data in the tropics, in terms of the magnitude and spatial consistency of climate variance across interannual to centennial timescales.

Laepple, T., and P. H. Huybers, 2014: Ocean surface temperature variability: Large model–data differences at decadal and longer periods. Proc. Natl. Acad. Sci. USA, 111, 16 682–16 687, https://doi.org/10.1073/pnas.1412077111.

Page 3, lines 5-6: please see general comments in previous section- why were the bulk of the CMIP5/PMIP3 Last Millennium simulations excluded? Analysis of results would appear much more robust if an attempt is made to present more than 1/3 of the Last Millennium simulations, or if reasoning can be given why the other simulations were excluded. Also, what is the cutoff used for a drift that is 'too strong'? Is this a global or local drift? All the CMIP5/PMIP3 past1000 simulations appear to show some sort of trend/drift at many grid points- the question is what is too much for the purposes of this AMO/PDO teleconnection study. Please clarify.

Reply: This comment has been addressed under the first "Main Concerns" earlier: we have extended our analysis to include four more models CSIRO, HadCM3, MRI and IPSL and revised the manuscript to include these models and compare the additional results.

Our decision to exclude three CMIP5 models (MIROC-ESM, FGOALS-s2 and GISS) was based on the results discussed in Atwood et al. (2016), Fleming and Anchukaitis (2016) and Bothe et al. (2013). This is mentioned in our original manuscript. Atwood et al (2016) and Bothe et al (2013) discussed long-term drift in global mean surface air temperature in their PI simulations. Similarly, Fleming and Anchukaitis

(2016) found drift in the Last Millennium simulations, which are apparent in the initial several centuries and excluded from their PDO analysis.

Page 3, Line 20: please see general comments in previous section- removing one linear trend over the full 1850-2005CE time period seems like it may add in low-frequency variability, and I am still not even sure why the historical simulations have been included if the focus is on the impact of volcanic eruptions in the pre-historical simulation time period.

Reply: This comment has been addressed under the second "Main Concerns" earlier. Our findings are not sensitive to this choice and we explain this in the revised manuscript. Our focus is broader than just the impact of volcanic eruptions, we are interested in the influence of external forcings in general on the diagnosis of the role of internal variability from observational evidence. During these simulations, volcanic forcing plays a major role so we did some additional analysis of that but it is not our only result.

Page 4, Line 8: 'we don't see much differences'- this is a subjective statement. What criteria are used? Perhaps something like a pattern metric or Euclidean distances metric could be used to say something more quantitative?

Reply: we revised this sentence to be less subjective, noting which key features (position and strength of the loading maxima and loading gradients) of the PDO patterns are present in the simulated and observed fields.

Page 4, Line 10: Please explain how the TAS time series is made- I assume annual mean (Jan-Dec?) temperature at each grid box, latitude-weighted, and masked ocean grid boxes? Over what latitude and longitude range is this area average made (is it the whole region used in the maps in the figures showing East Asia?)? Please provide more details in the text.

Reply: For the TAS time series, the annual mean (Jan-Dec) TAS is calculated over the land grid points only and area averaged over the region 60E -150E and 10N-55N. We added this additional information to the revised manuscript.

Page 5, line 5-7: There are other PDO reconstructions- fine to not include them, but can you state why this one is selected over others?

Reply: We have used the selected PDO reconstructions based on the availability of the data for a longer period that covers at least 1000 years of our main analysis period 850-2000. The revised manuscript now states this selection criterion.

Page 5, lines 11-15: As far as I can tell, the model-based PDO indices are made from monthly data, and the paleo-based PDO indices are made 'annual' data (or seasonally sensitive proxy records)- would a

better comparison be to make annual means of SAT for the model data, then construct the PDO index, so the index is more comparable to the annual proxy-based index? (or can you show that the annual and monthly modelbased PDO patterns and time series are similar?).

Reply: The model simulated monthly mean SST data were, in fact, already converted to annual mean data before applying the EOF analysis to get the PDO pattern and its time series (i.e. as suggested by the reviewer – we now make this clear by adding 'annual-mean SST anomalies' to the Fig. 2 caption). We have done this because all our analysis is based on the annual mean data, which also compares with the annual mean reconstructed data. We have also confirmed that model based PDO patterns for annual and monthly data are similar (see figure R7 of our reply in the interactive discussion).

Page 5, Line 21, line 25: The 90% significance level seems oddly low, and arbitrarily used in only certain cases- do your results consistently pass a 95% significance test (both the regions in the maps and the spectra)? For example, the 'significant' spectral peaks in Figure 10 appear quite close to the 90% significance level- if you made this a 95 or 99%, are these 'significant spectral peaks' at all significant?

Reply: Please see our response to "main concern (4)" above.

Page 8, line 26: the authors discuss a weak response in BCC to volcanic eruptions- is this a finding that has been noted previously (e.g., Driscoll et al., JGR, 2012, or some sort of similar CMIP5 comparison to observations?)? How realistic is this model's response relative to the other models' responses to volcanic eruptions (especially compared to observations of more recent eruptions and their impacts)? I ask because this difference seems to be important to the results- for example, should the BCC changes (or lack thereof relative to the other models) in PDO, AMO, and associated teleconnections with E Asia be viewed as just as realistic as the other models' responses? Or is it an outlier because it doesn't respond at all to volcanic eruptions when it should?

Reply: By analysing the CMIP5 *historical* simulations, Driscoll et al. (2012) found largest anomaly in the reflected SW radiation in the BCC model. Here, we show that the weak response in BCC to volcanic response only exists in the *last millennium* simulations, where we have analysed three major volcanic eruptions that happened in the last millennium. We also analysed the same for the major volcanic events during the historical period but didn't find such weak response in BCC model compared to the other models. So, it seems that the weak volcanic forcing and response in BCC GCM only exist in its last millennium simulation.

Page 9, Line 25-26: It would be helpful to show results from the other four CMIP5 Last Millennium simulations here to put these results in context- right now, 1/3 of the models show a completely different result, but this '1/3 of models' is just the BCC model.

Reply: As noted earlier, we now analyse four other models and it has improved our manuscript.

Page 9, Line 26-29: Would this result imply that the models show an unrealistically large response to eruptions? Or that there is too little internal, low-frequency variability (e.g., Laepple and Huybers)? Or does this suggest both, or something else?

Reply: The potential reasons for the stronger volcanic signal in some models compared with some reconstructions are varied and could include those stated by the referee alongside other reasons (notably errors and biases in the reconstructed temperatures, AMO, PDO and/or forcing histories). We prefer not to over-speculate at this point and instead present the findings.

Page 10, line 2-3: the authors state that 'all models display red spectra'- in the methods (and in the time series in the figures), it seems that the data have been low-pass filtered, so by definition, the high-frequency variability has been reduced relative to the low-frequency variability (thus reddened)- I'm not sure that 'redness' really means anything in this case. If 'redness' does mean something after the data have been filtered, or if the data have not been low-pass filtered before spectral estimation, please clarify/explain- for example, if the authors mean to say that one model has more lowfrequency variability than another, that may be more accurate.

Reply: The data have **not** been low pass filtered before spectral estimation. We have now clearly mentioned this in the revised manuscript.

Furthermore, the 'pronounced multidecadal variability' barely surpasses the 90% significance threshold, as do most of the 'significant' peaks referenced in this paragraph.

Reply: As noted above, the presence of individual periodicities is of less interest than the overall shape of the spectra (to repeat here for convenience, we are interested in: "the overall shape of the spectra, their redness and broad multi-decadal power, and whether these are similar between models, with/without forcing, and between AMO index definitions"). This paragraph discusses some of these features and not individual significant periodicities, so it is not affected by the choice of the significance threshold. We have removed the significance lines to avoid this confusion.

These power spectra (AMO and PDO power spectra figures) are shown without any error bars- when the spectra are compared and declared similar/different, some sort of spectral estimation confidence bound/error bar on the figure could show if these differences fall within the confidence bounds of the spectral estimates.

Reply: We cannot add individual confidence intervals to each individual spectrum, especially now that there are seven GCMs, without obscuring the message of the diagram by two many lines. Using a log-scale for the y-axis would mean that a single confidence interval could be marked that applies to all frequencies but we decided not to do this because (a) a single confidence interval would only apply to all series if they are based on the same length timeseries (which is not true for the PI runs, though it is for

the LMH runs) and (b) we tried using a log-scale and felt that it made it harder to see the differences between the GCMs.

Page 10, Lines _5-15: Perhaps this is the first time that this analysis has been done, but I would be surprised- has anyone else compared the power spectra across these simulations before? For example, Cheung et al., (2017) compares instrumental-based AMO and Pacific variability to CMIP5 historical simulations (and also how the spatial patterns associated with these modes can change through time). Parsons et al., 2017 (J Clim) compares instrumental, AR1, and CMIP5 Last Millennium, and CMIP5 Control spectra over the North Pacific and North Atlantic, and Fredriksen and Rypdal (2016, J Clim) compare spectra over ocean basins in CMIP5 models.

Reply: As per our understanding, we didn't find any study that compared the power spectra across the simulations in detail. As the reviewer mentioned, Parsons et al. (2017) discussed the power spectra in terms of ensemble mean of CMIP5 models but not the details of the power spectrum of individual CMIP5 models. Similarly, Cheung et al. (2017) did mention the power spectrum of ensemble mean for the historical period and not the details of the individual members nor the last millennium runs. Fredriksen and Rypdal (2016) compared the power spectrum of CMIP5 control runs with instrumental records but did not compare with last millennium simulations. So, we focused on the power spectra of individual CMIP5 models used in our study and compare the results between control and last millennium simulations.

Page 10, Line 23: the authors claim that the spatial patterns of AMO and PDO are similar to the patterns from observations. I see no comparisons among modelled and observed spatial patterns of variability. In fact, it would be helpful if the authors would show the spatial patterns from observations (of course acknowledging that the instrumental-based data have their own limitations) in Figures 1 and 2- this would help put the model results in context.

Reply: We have added the spatial patterns of AMO and PDO using observation data (Fig. 1 and 2).

Page 10, line 25: again, it's unclear if the data have been low-pass filtered before spectral analysis. Also, see my above comments- saying the spectra are 'red' seems meaningless if the data have been low-pass filtered. Again, the significant peaks barely surpass a 90% threshold- please discuss or mention if this significance is sensitive to threshold level.

Reply: The data have not been low pass filtered before the spectral analysis. We make this clear in the revised manuscript.

Also, as stated above it would be good to include error bars/lines on the spectra to know if the 'significant' differences from the background spectrum significant given uncertainties in the power spectral estimation?

Reply: See earlier response.

Page 11, _Line 25: good point.

Reply: Thank you.

Page 12, _line 4: OK, so other recent methods have been used to reconstruct SAT fields (e.g., Last Millennium Reanalysis from Hakim et al., 2016, JGRA and Tardiff et al., in review at CP)

Reply: We will cite the most recent Last Millennium Reanalysis paper and note that this does provide a surface temperature field that could be used to define an index based on the difference between the regional and global SST (though it is not independent of the climate model used to produce the reanalysis, so there may be some circularity in using the resultant AMO reconstruction to evaluate climate model behaviour).

Figures:
Figures 1, 2, 3, 5: please include panels showing similar analyses from instrumental-based data products.

Reply: We have now included panels based on the data from the instrumental period for Fig1 and 2. We have not included the instrumental data analysis for Figure 3 and 5, because the data length is not enough to calculate the correlation which is based on 30-year low pass filtered data.

Figure 4, Figure 6: it is interesting to see the PDO-E Asia and AMO-E Asia differences, but it would be nice to see some confidence bars on the control run values. For example, Coats et al. 2013 show that teleconnections can change from century to century. Could you do some sort of running correlation or subsample the control run to see how variable this E Asian relationship is (or is there enough data?)

Reply: We considered using confidence intervals instead indicating the statistical significance (which occurs when the confidence interval does not include zero) but now that we extended our analysis to seven GCMs it is problematic to fit all the information without obscuring the individual model results. A running correlation or equivalent is not appropriate here because we are working with 30-year smoothed data (so that we can assess multi-decadal variability rather than the interannual variability that Coats et al., 2013, considered) and dividing it century by century would leave insufficient independent 30-year samples in each century.

Figure 9: Is there a way to put these results in context? For example, if you include the post-Pinatubo response in these models, could you show how the models compare to obs? Which models are more realistic? (CCSM4/MPI or BCC?)

Reply: The issue with BCC appears to be confined to the Last Millennium simulation and not to the Historical simulation, so a comparison with observations post-Pinatubo would not help.

Figures 10 and 11: inclusion of instrumental-based spectra could be helpful here too how realistic are these reconstructions?

Reply: We have included the instrumental based spectra although the data length is short.

Compact listing of purely technical corrections (typing errors, etc.).

Page 1, Line 13: 'and their spectral characteristics'- remove 'their'
Page 3, line17: change sentence to: 'Each model version was the same across all the simulations.'
Page 4, line 8: 'much differences'- please re-word (e.g., 'A pattern correlation statistic shows minimal differences among : : :'
Page 5, Line 7: 'largely suffer from the influence of external forcing'
Page 6, Line 4: 'no time-varying (transient?) external radiative forcing'
Page 6, line 31: 'This situation is equivalent to (that?) of Fig.' – there appears to be a missing word here
Page 7, Line 13-15: 'in the southern parts': : :'in all three models': : :'with the strongest correlation in the northeast region'
Page 7, line17: 'though it varies'
Page 9, Line 10: the sentence starting with 'Despite' appears a bit awkward- suggest rewording.

Reply: Thank you for the careful checking – we have addressed these minor technical/wording errors in our revised manuscript.

Identifying teleconnections and multidecadal variability of East Asian surface temperature during the last millennium in CMIP5 simulations

Satyaban B. Ratna[1], Timothy J. Osborn[1], Manoj Joshi[1], Bao Yang[2], Jianglin Wang[2]

[1]Climatic Research Unit, School of Environmental Sciences, University of East Anglia, Norwich, NR2 2BP, United Kingdom
[2]Key Laboratory of Desert and Desertification, Northwest Institute of Eco-Environment and Resources, Chinese Academy of Sciences, Lanzhou, 730000, China

Correspondence to: Satyaban B. Ratna (s.bishoyi-ratna@uea.ac.uk)

Abstract. We examine the relationships in models and reconstructions between the multidecadal variability of surface temperature in East Asia and two extratropical modes of variability: the Atlantic Multidecadal Oscillation (AMO) and the Pacific Decadal oscillation (PDO). We analyze the spatial, temporal and spectral characteristics of the climate modes in Last Millennium, Historical and pre-industrial control simulations of ~~three~~seven CMIP5/PMIP3 GCMs, to assess the relative influences of external forcing and unforced variability. These models produce PDO and AMO variability with realistic spatial patterns ~~and their~~but widely varying spectral characteristics. AMO internal variability ~~strongly~~significantly influences East Asia temperature in ~~one model (bcc-csm1-1~~five models (MPI, HadCM3, MRI, IPSL and CSIRO), but has a weak influence in the other two (BCC and CCSM4~~ and MPI-ESM-P~~). In ~~all three~~most models, external forcing greatly strengthens these statistical associations and hence the apparent teleconnection with the AMO. PDO internal variability strongly influences East Asian temperature in two out of ~~the three~~seven models, but external forcing makes this apparent teleconnection much weaker. This indicates that the AMO-East Asian temperature relationship is partly driven by external forcing whereas the PDO-temperature relationship is largely ~~driven by~~from internal variability~~. External~~ within the climate system. Our findings suggest that external forcing confounds attempts to diagnose the teleconnections of internal multidecadal variability. Using AMO and PDO indices that represent internal variability more closely and minimising the influence of external forcing on East Asia temperature can partly ameliorate this confounding effect. Nevertheless, these approaches still yield differences between the forced and control simulations and they cannot always be applied to paleoclimate reconstructions, so we recommend caution when interpreting internal variability teleconnections diagnosed from reconstructions that contain both forced and internal variations.

1 Introduction

Coupled ocean-atmosphere processes cause climate variations on interannual to multidecadal timescales (Dai et al., 2015 and Steinman et al., 2015), resulting in persistent temperature and hydroclimate anomalies over both adjacent continents and remote regions (Wang et al. 2017; Coats and Smerdon, 2017), potentially having both immediate and long lasting consequences

for society (Büntgen et al., 2011). Assessing teleconnections between ocean and land can be done using a number of methods, each of which have their limitations. The usefulness of the observational record for understanding multidecadal teleconnections is limited by its length. Paleoclimate reconstructions can provide information on longer time scales, and can also place the current climate regime in a long-term perspective. Several reconstructions of modes of climatic variability such as the Atlantic Multidecadal Oscillation (AMO) and the Pacific Decadal Oscillation (PDO) have been attempted using networks of proxy data, including tree-~~ring~~rings, ice cores, speleothems, coral growth, lake sediments, and documentary evidence (e.g. MacDonald and Case, 2005, Mann et al, 2009, Wang et al, 2017, Fang et al. ~~2018b~~2018, Wang et al. 2018). However, limitations in the geographic and temporal coverage of the proxy records, including terrestrial and marine locations, and differing climatic and seasonal sensitivities, affect the ability of these reconstructions to fully represent decadal to centennial variability (Jones et al, 2009; Christiansen and Ljungqvist, 2017; Smerdon and Pollack, 2016; Jones and Mann, 2004; Frank et al., 2010).

Global climate model (GCM) simulations can offer complementary long-term perspectives on the behaviour of important modes of climate variability (Atwood et al, 2016; Fleming and Anchukaitis, 2016; Landrum et al, 2013). Such models can also be used to identify the extent of large scale teleconnections between these modes and regional climate (Coats et al., 2013). GCMs also provide a means of separating changes associated with external forcing from those arising by internal variability since they can be run using differing boundary conditions (Schurer et al., 2013, 2014). Atmosphere-ocean coupled GCMs with more extensive representation of processes within the climate system ~~components~~ also permit more detailed examination of spatial and temporal variations during the last millennium. However, similar to proxy based records, there are also limitations in paleoclimate simulations. Laepple and Huybers (2014) found potential deficiencies in Coupled Model Intercomparison Project Phase 5 (CMIP5) SST variability, with model simulations diverging from a multiproxy estimate of SST variability (that is consistent between proxy types and with instrumental estimates) toward longer timescales. Parsons et al. (2017) found very different pictures (in terms of the magnitude and spatial consistency) of natural variability between the CMIP5 models, including in the North Atlantic, and between models and paleoclimate data in the tropics.

The focus of our study is on the annual mean temperature of East Asia on multidecadal and longer timescales. On these timescales, variability associated with the AMO (Schlesinger and Ramankutty, 1994; Kerr, 2000; Delworth and Mann, 2000; Wang et al. 2017) and the PDO (Mantua et al. 1997; Newman et al., 2016; Buckley et al., 2019) can exert an important influence on the climate over Asia (Qian et al. 2014; Wang et al. 2013~~; Dong 2016~~, 2018; Li et al. 2017; Fang et al. ~~2018a~~2019). Our aims are to: (1) identify the key teleconnections between the AMO, PDO and East Asian temperature in climate models; (2) to determine ~~how~~to what extent external forcings affect these simulated teleconnections; (3) contrast the simulated and reconstructed behaviour of East Asian temperatures on multidecadal timescales; (4) develop recommendations for making

unbiased comparisons between model ~~data~~output and paleoclimate reconstructions. We also provide insight into the long-term simulated behaviour of these modes of climate variability with respect to ~~the~~ external forcing and internal variability.

The rest of the article is organised as follows: Section 2 describes the climate models and paleoclimate data used in this study, and the methods to calculate the climate indices. Section 3 describes the results associated with AMO and its teleconnection with East Asian surface temperature and Section 4 discusses the results associated with the relationship between PDO and East Asian surface temperature. The role of volcanic forcing on these aspects of climate variability is demonstrated in Section 5. In Section 6, further results are discussed and conclusions are summarised.

2 Data and Methods

2.1 Climate model simulations

We select models from the Coupled Model Intercomparison Project Phase 5 (CMIP5; Taylor et al. 2012) that had provided output for all three experiments considered here: (i) pre-industrial control (~~PC~~PI) run with constant external forcing, (ii) Last Millennium (LM) and (iii) Historical experiments ~~(HIST)~~ with external forcings. Of the ~~six~~ten GCMs that met this criterion, three models (MIROC, FGOALS, GISS) were excluded because they show a strong drift in the ~~last millennium~~LM or ~~control~~PI simulations (~~Artwood~~Atwood et al. 2016, Fleming and Anchukaitis, 2016; Bothe et al., 2013). Atwood et al (2016) and Bothe et al (2013) found long-term drift in global mean surface air temperature in some PI simulations, while Fleming and Anchukaitis (2016) found drift in some LM simulations during the initial several centuries and excluded these from their PDO analysis. Details of the remaining ~~three~~seven GCMs are summarised in Table 1 including the volcanic and solar forcings used. The forcing and boundary conditions for the LM simulations follow the protocols of Paleoclimate Model Intercomparison Project Phase 3 (PMIP3) as discussed by Schmidt et al. (2011) and Schmidt et al. (2012). The forcings are composed of volcanic aerosols, solar radiation, orbital variations, greenhouse gas (CH_4, CO_2, and N_2O) concentrations, and anthropogenic land-use changes over the period 850-1849. The ~~HIST~~Historical simulations are forced with natural and anthropogenic forcing over the period 1850-~~2005~~2000.The comparison of these 'forced' simulations with 'unforced' control simulations provide a means of assessing what portion of the variability is attributed to external forcing and what portion reflects purely internal variability. Also, these simulations are useful in providing a longer term perspective for detection and attribution studies.

We interpolate output from the ~~BCC and MPI~~all the models to the CCSM4 grid resolution to facilitate intercomparison. We note that the available model simulations were not necessarily continuous from their LM simulations into their ~~HIST~~Historical simulations, so modes of variability cannot be calculated across 1850. Each model version was the same across ~~the~~ all the simulations. Since our focus is on natural variability arising from internal and external causes, we have minimised the influence of any residual long-term drift or of anthropogenic transient forcings ~~in the GCM simulations~~ by first detrending (removing

the linear trend) ~~across~~ the ~~Last Millennium~~LM (850-1849) and ~~historical~~Historical (1850-2000) time series separately and then merging them into a continuous detrended timeseries for the period 850-2000 (LMH hereafter). Our results are not sensitive to the linear detrending of the Historical simulations (see Supplement Figs S1 and S2).

2.2 Diagnosing Atlantic and Pacific variability

The AMO and PDO timeseries are diagnosed using the same methods for both the model simulations and the instrumental observations. For the latter we used HadISST (Rayner et al, 2003) and ERSST (Smith and Reynolds, 2004) for the periods 1871-2000 and 1854-2000, respectively.

The AMO index is calculated from the area-weighted North Atlantic (~~80W – 0W,~~80– 0~~–65N~~°W, 0–65°N) monthly mean SST anomaly for the LMH and ~~PC~~PI simulations. When the value of the index is positive (negative), it is known as the warm (cold) phase of the AMO. We have considered here two sets of AMO indices, both with (hereafter, ~~AMOrem~~AMOr) and without (hereafter, ~~AMOnorem~~AMOnr) first subtracting the global mean SST anomaly time series (Trenberth and Shea, 2006) from the spatially averaged (North Atlantic) time series anomalies at each time interval. Atlantic SST will exhibit both internal variability and the response to external forcings~~:~~ (Wang et al. 2017): by subtracting the global-mean SST anomaly, the ~~AMOrem~~AMOr index will reflect more closely the variability that is focussed on the North Atlantic region and not the signal of external forcing present in the global SST pattern. The annual mean of the AMO indices generated by the above two methods are regressed over the North Atlantic annual mean SSTs (Fig. 1) ~~which~~to shows the spatial pattern of the AMO~~.~~; they closely agree with the observations (Fig 1, bottom panel).

The PDO index is calculated as the leading mode from an empirical orthogonal function (EOF) analysis of ~~monthly residual~~annual SST anomalies in the north Pacific region 20-65°N and 110°E-110°W, which are calculated by first removing the long-term monthly means ~~and~~, then subtracting the monthly mean global SST anomaly at each time interval~~.~~ and then forming annual means. The EOF analysis yields spatial patterns (loadings) and temporal scores (time series). In its ~~warm~~/positive (~~cool~~/negative) phase, SSTs are above (below) normal along the west coast of North America and below (above) average in the central north Pacific (Fig. 2).~~We don't see much differences~~ The simulated PDO patterns agree well with each other and with the observed pattern (Fig. 2, bottom panel), in ~~the EOF~~terms of the position of strength of the loading ~~among the three models but there is~~maxima and main loading gradients. There are considerable differences in their time series, however, which are discussed later.

The model simulated AMO and PDO indices are generated using monthly mean SSTs for the LMH (850–2000) and ~~PC~~PI simulations, and then converted into annual mean (January-December) values for our analysis. ~~For~~Similarly, for the time series analysis for the temperature over East Asia (TAS), ~~we~~the annual mean (January-December) value is calculated over the land grid points only and area averaged over the region 60-150°E and 10-55°N. We also consider warm (April-September) and cold (October-March) season averages.

2.3 Paleoclimate and ~~volcanic~~ forcing reconstructions

The ~~BCC and CCSM4~~ GCMs used volcanic forcing from either Gao et al. ~~(2008, hereafter GRA) and MPI used volcanic forcing from~~(200) or Crowley et al. (2008, hereafter CEA) in their last millennium simulations (Table 1). Accordingly, we compare the model and reconstructed data with GRA and CEA, as well as ~~a~~with the newer volcanic forcing reconstruction from Sigl et al. 2015 (hereafter, SIG). Table 1 also lists the solar forcing reconstructions used to drive the GCMs (hereafter VSK, DB and SBF) and we use these to identify the solar signal in the data.

We used proxy-based reconstructions for the AMO, PDO and surface temperature over East Asia (TAS) as summarised in Table 2. We selected these reconstructions instead of alternatives because of the availability of the data for a period that covers at least 1000 years of our main analysis period 850-2000.

Two AMO reconstructions are used in this study. Mann et al (2009) reconstructed near-global fields of surface temperature using a diverse mix of annual and decadal resolution tree-ring, coral, ice core and sediments records from across the globe. Their AMO series (hereafter AMN09) was computed from the North Atlantic SST grid cells of their reconstructed fields and extends for the period 500-2006 with 10-year low-pass filters. The annually resolved AMO by Wang et al (2017) is based on tree ring, ice core, historical records only from circum-Atlantic land regions and is available for the period 800-2010. Wang et al. (2017) first reconstruct Atlantic Multidecadal Variability (hereafter WN17V) and then subtract an estimate of the externally-forced component to obtain a series that represents mostly internal variability, denoted the Atlantic Multidecadal Oscillation (hereafter WN17O). The two ~~AMO~~ reconstructions ~~(~~AMN09 and WN17V~~)~~ provide estimates of the full (both external and internal) variability of the North Atlantic SST. Although Mann et al. (2009) reconstructed near-global SST fields, we have not subtracted the global-mean SST from the Atlantic-mean SST to isolate the *internal* AMO variability (cf. the '~~AMOrem~~'AMOr' series from the models) because prior to 1600 their reconstruction is a linear combination of only two spatial patterns which gives limited information about the Atlantic–global SST difference. Wang et al (2017) did attempt to isolate the internal variability by regressing against solar and volcanic forcing reconstructions, to yield the WN17O series also considered here.

One annual mean PDO reconstruction is based on Mann et al (2009) as described above and hereafter denoted as PMN09. This series is an average of SST grid cells over the central north Pacific region (22.~~5°N~~5–57.~~5°N~~5°N, 152.~~5°E~~5°E–132.~~5°W~~5°W):

since this region has mostly negative loadings in our EOF-based PDO index (Fig. 2), we multiply PMN09 by minus one to make it comparable to the other PDO indices. Another annually resolved PDO index is from MacDonald and Case (2005; hereafter, MD05) who used only tree ring records from *Pinus flexilis* in California and Alberta to reconstruct PDO for the period 993-1996. The PDO reconstructions, unlike the EOF-based definition in modeled and observed SST ~~dataset~~datasets, might also contain some signal of external forcing because the proxy records~~, used in reconstructions, largely suffer from influence of external forcing~~ are influenced by externally-forced variability.

The East Asian temperature reconstruction for the warm season is from Wang et al. (2018, hereafter WN18), which uses the mean of seven published reconstructions and is available for the period 850-1999. See Wang et al. (2018) for a discussion of the underlying reconstructions and their similarity/differences. We repeat some of our analyses with three of the individual reconstructions used in the WN18 composite (see Supplement Fig. S3).

It should be noted that the time sequences of the reconstructed and simulated data are not directly comparable because each will have its own realisation of internal variability. They should, however, be internally consistent so that their teleconnections can be compared on multidecadal time scales, along with any contribution that is externally forced (to the extent that the external forcing matches between the datasets).

2.4 Analysis methods

Since our focus is to understand climate variability on multidecadal timescales, all the time series are passed through a 30-year low pass filter using the Lanczos filter. The correlation analyses are tested for statistical significance using the two-tailed student's t-test. The number of degrees of freedom are the number of 30-year long segments minus 2, i.e if low pass filtered 1000-year long time series has 33 independent samples (1000/30) and 31 degrees of freedom. ~~The corresponding critical correlation value is used to test the statistical significance at 90% or 95% level.~~ The null hypothesis (that the correlation is zero) is rejected if the correlation value is greater than the ~~critical correlation value~~corresponding critical value: we test the statistical significance at the 95% level for area-means but lower this to 90% at the grid-cell level because additional noise increases the risk of a type II error.

Spectral analysis ~~to identify the spectral shape and any major periodicities~~ of AMO and PDO indices is performed via the Fast Fourier Transform (FFT). ~~The~~In undertaking spectral analysis, we are interested in the overall shape of the spectra, their redness and broad multi-decadal power, and whether these are similar between models, with/without forcing, and between AMO index definitions. We are less interested in the apparent statistical significance of ~~the spectra was tested against~~individual periodicities so we do not apply such a ~~red noise background (Mann and Lees, 1996) and the periodicities at multidecadal time scales that are significant at 90% level are emphasized.~~statistical test. In order to isolate the near-internal variability from the

LMH model runs, in some analyses we regress out the influence of volcanic forcing from the TAS, AMO and PDO timeseries by calculating the regression coefficient of the GRA or CEA volcanic global forcing timeseries against the TAS, AMO and PDO time series, respectively.

3. Influences of Atlantic Multidecadal Oscillation

Figure 3 shows the correlation between the AMO index and multidecadal variations in surface temperature in the LMH and PCPI simulations. The correlation with *area-averaged* East Asia surface temperature (TAS) is also calculated (Fig. 4). In the PCPI simulations with noconstant external radiative forcing, internal climate variability alone results in correlations between the AMOAMOnr and East Asian temperature that are generally positive (Fig. 3a, b, c), though only the MPI model shows widespread statistically significance on a point by point basis (Fig. 43, column 1) – i.e. a warmer North Atlantic Ocean is associated with warmer East Asian temperatures. There is only widespread statistical significance on a grid-cell basis for four models (MPI, HadCM3, IPSL and CSIRO; Fig. 3, column 1), though correlations with area-averaged TAS are quite strong (multi-model mean > 0.5) and statistically significant for all models except BCC and CCSM4. The strength of the correlation is very sensitive to the presence of external forcing, becoming more strongly positive both spatially (Fig. 3g, h, i) and on an area-averaged basis (Fig. 4) in the LMH run (i.e. increasing from 0.32, 0.29for all GCMs (all are significant and 0.71 for the BCC, CCSM4 and MPI PC runs respectively, to 0.62, 0.85 and 0.84 in the LMH run). For all the threemulti-model model correlation reaches 0.75). In many models, the strong positive correlation occursoccur mostly because natural external (e.g., volcanic eruptions) forcings cause concurrent warming or cooling in both the Atlantic and East Asian regions (Fig. 7).7). Indeed, including external forcings changes CCSM4 from having the weakest (and non-significant) correlation to having the strongest (0.84) correlation between the AMOnr and E Asian temperature.

When we remove the global SST anomaly before calculating the AMO index, its association with TAS becomes much weaker,. The reduction in correlation is especially large for LMH runs, as shown in both on a grid-cell basis (Fig. 3(j, k, l, column 3 vs g, h, i. 4), and for area-averaged TAS (Fig. 4 AMOrem, AMOr vs AMOnorem.AMOnr). This is because much of the external forcing influence on N Atlantic SST also drives global SST, so subtraction of the global-mean SST anomaly prior to the calculation of the AMO removes this externally-forced variability from the AMO. However, because TAS has a different sensitivity to global forcings such as volcanic eruptions, the , its correlation with AMOr is decreased, rather than falling to insignificant values. For but remains significant for some models (MPI, MRI and CSIRO). Comparing the correlations with the MPI model, there is a clear association between the AMO and East Asian temperaturesAMOr index, we see that is generated by internal variability, especially in the northern half of the region considered here, since a positive the correlation occurs even in the PC run (Fig. 3c and f). This remains even if the global SST anomaly is subtracted, suggesting that this mode of internal variability only partly projects onto global mean SST anomalies. If the AMOrem index is used, then the correlation

~~is~~is notably weaker in the LMH run than in the ~~PC~~PI run for the MPI~~-model.~~, HadCM3 and IPSL models (Figs. 3 and 4). This is because the forcings generate a response in the TAS but not in the ~~AMO~~AMOr (any response is mostly removed because global SST is subtracted from Atlantic SST), weakening their correlation. ~~This behaviour is not seen in the other two models because the AMOrem index has little correlation with TAS even in their unforced PC runs~~MRI and CSIRO are notable in that their TAS correlations with AMOr are stronger in the LMH run than in the PI run; this could arise if the amplitude of SST response is greater in the Atlantic than in their global mean, so that AMOr still retains an external forcing signal that then correlates with the external forcing signal in E Asian TAS.

In summary, four models show a clear association between the AMO and East Asian temperatures (especially in the northern half of the region considered here) that arises from internal variability (i.e. in the PI run) that remains significant even if the global SST anomaly is subtracted. This suggests that this mode of internal variability only partly projects onto global-mean SST anomalies. Furthermore, the correlations for all models are strongly affected (increased) by the inclusion of external forcing unless the AMO is defined by subtracting the global-mean SST from the Atlantic SST.

These dependencies of the model correlations on the presence of external forcing and on the calculation of the AMO index are important in the context of interpreting reconstructed data. Suppose we wish to use reconstructed data to answer the question "does the AMO, as a mode of *internal* variability, influence E Asian temperatures on multidecadal timescales?" The reconstructions represent the real world (a situation with external forcings) and some AMO reconstructions (e.g. AMN09 and WN17V) have not isolated internal variability of the N Atlantic SST from externally-forced signals (because, for instance, global-mean SST cannot be subtracted before calculating the AMO if global SST has not been independently reconstructed). This situation is equivalent to column 3 of Fig. ~~3g, h, i~~3 (LMH runs with ~~AMOnorem~~AMOnr indices) and a strong positive correlation might be found between the AMO and E Asian temperatures – but this would *not* establish that the AMO, as a mode of internal climate variability, was strongly influencing E Asian temperatures on multidecadal timescales.

The WN18 E Asian reconstruction represents *warm-season* temperature, so we repeated our model analysis but using both warm and cold season temperatures and obtained results that are closely consistent with those using annual-mean temperatures. The reconstructed AMO series all show positive correlations with the WN18 E Asian temperature reconstruction (Fig. 4). Those representing full AMO variability (WN17V and AMN09) have correlations around 0.4, while the correlation with E Asian temperature falls ~~towards~~to 0.24 (which is not significant) for the WN17O series representing only internal AMO variability.

None of the reconstructed AMO or E Asian surface temperature series correlate significantly with the equivalent simulated series from the LMH runs, indicating that internal variability and any errors in reconstructed climate and forcings dominate the influence of external forcing, or that model response to forcings is unrealistic.

4. Influences of Pacific Decadal Oscillation

Similar to the AMO analysis, Figs 5 and 6 show the correlation between PDO and TAS. The PDO is ~~mostly~~ negatively correlated with TAS ~~except for a small region~~ in ~~southern parts of India and Southeast Asia in all the three models, with the correlation being strongest in the north east of the region (Fig. 5). This is~~Japan, as expected because cooler SSTs lie adjacent to this region when the PDO index is positive (Fig. ~~2). The correlation between the PDO and TAS is therefore~~2). These negative~~,~~ correlations extend from Japan across large parts of the north east of our region in four (BCC, CCSM4, IPSL and CSIRO) out of seven models, though ~~varying~~they vary widely in strength and significance between ~~the~~ models ~~especially for the PC~~, and are mostly weakened by the inclusion of external forcing (LMH cf. PI in Fig. 5). Most models (for both the PI and LMH runs ~~(see)~~ show a dipole with mainly negative correlations in the north or centre of our region and positive correlations in the south (e.g. parts of India and Southeast Asia). The predominance of negative correlations across the spatial field means that six out of seven models simulate a negative correlation between area-averaged TAS and PDO, though few are significant because we are averaging across regions with opposite correlations (Fig. 6). ~~These~~There are two key differences between the results with and without external forcing. First, the correlations weaken when external forcing is applied to the models (except for the MPI model where it was already weak~~), suggesting that external~~). Second, the spread in results is much wider in the absence of forcing (with significant negative correlations for BCC and CCSM4). Together, these results suggest that the internal-variability teleconnection between PDO and E Asian temperature is very model dependent but that external forcing consistently weakens the association. The weakening is likely because the forcing drives additional variability in East Asian temperatures but not in the PDO (because we subtract the global-mean SST anomaly prior to calculating it, and use an EOF definition that depends on SST spatial differences rather than mean SST across the North Pacific, Fig. 2). Using this definition (rather than a simple area-mean SST), the model PDOs do not have strong or consistent responses to forcing in the LMH simulations, in agreement with Landrum et al. (2013) and Fleming and Anchukaitis (2016).

We have also compared the reconstructed PDO and TAS time series (Fig. 6). The correlations are also negative: MD05-WN18 and PMN09-WN18 are -0.10 and -0.41, respectively, ~~and~~but only the latter is significant. The weak correlation with MD05 might be partly related to the fact that this reconstruction is based on only two tree-ring records of North America, suggesting ~~a possible~~more uncertainty if teleconnection patterns it ~~relied~~relies on change through time. The simulated PDO series show very weak correlations with the reconstructed PDO series: as with the AMO, this implies that an external forcing influence is weak compared with internal variability and reconstruction errors, or that models' PDO response to forcings is unrealistic. For the simulated PDO indices, any external forcing influence may be weak if the PDO calculation (an EOF analysis with the global-mean SST removed) effectively removes a forcing signal. As before, we repeated our model analysis using both warm and cold season E Asian temperatures and found very similar results to the annual temperatures.

5. Effect of volcanic and solar forcing

The behaviour of the AMO and PDO timeseries and their correlation with E Asian temperature are clearly sensitive to the presence of external forcing (e.g. LMH versus ~~PC~~PI differences), so we now consider the effect of volcanic and solar forcings. Volcanic forcing~~ is~~ is the largest external influence within the ~~Last Millennium~~LM runs (Atwood et al. 2016~~). Previous studies indicated that~~) and is a key driver of the Little Ice Age and other cooling periods during the last millennium ~~are largely driven by volcanic forcing~~ (Briffa et al. 1998; Ammann et al. 2007; Atwood et al. 2016). ~~All~~However, Wang et al. (2018) showed that their E Asian temperature reconstruction has significant multidecadal correlations with solar forcing reconstructions. So, we have compared the model simulations and reconstructions to both volcanic (GRA, SEA and SIG; Fig. 7a) and solar forcing (VSK, DB and SBF; Fig. 7b). All three volcanic forcing timeseries (GRA, CEA and SIG) are closely correlated with each other but are by no means identical (Fig. 7a). For the period A.D. 850-2000, their correlations ~~are~~range from 0.75 ~~(~~to 0.82 (for pairs of GRA~~ and,~~ CEA~~), 0.81 (GRA~~ and SIG~~)~~ volcanic forcing) and from 0.80 to 0.91 (for pairs of VSK, DB and ~~0.82 (CEA and SIG~~SBF solar forcing), highlighting the value in considering multiple forcing histories.

~~The~~ Visually, it is clear to see that the simulated E Asian temperatures and AMOnr timeseries ~~for CCSM4 and MPI~~ display a ~~strong~~multidecadal association ~~between~~with volcanic forcing, while AMOr and ~~model simulated TAS and AMO (~~PDO timeseries do not (Fig. 7~~), confirmed by the correlations (Fig. 8). These models simulate a significantly~~). The colder climate over East Asia ~~in response to volcanic forcing compared to BCC, which~~and the Atlantic (i.e. AMOnr) is especially evident during the three periods containing strong eruptions (~~1257/8, 1458/9~~1250s, 1450s and ~~1815). The case is same for the AMOnorem time series, with the models simulating cold Atlantic SST anomalies during the periods~~1810s). Potential influences of ~~strong~~ solar forcing are harder to identify because the forcing is weaker and shows less distinct episodic behaviour than the volcanic forcing. Turning to correlations (Fig. 8) some key behaviours are clear.

First, simulated E Asian temperature is positively correlated with volcanic ~~eruptions, with high correlations for CCSM4 and MPI ranging from 0.49 to 0.73 with~~ forcing (significant for all models except BCC) but this is not the case for reconstructed temperatures (on these multidecadal timescales at least; WN18 also report that the volcanic signal is small compared with other influences). We tested to see if the latter result was due to our use of the Wang et al. (2018) composite of reconstructions rather some individual reconstructions that might better resolve the response to volcanoes, but obtained similar results (Supplement Fig. S3). E Asian temperatures are also positively correlated with solar forcing but these are weaker than with volcanic forcing and are either insignificant or marginally significant for all models and reconstructions.

Second, simulated AMOnr timeseries are more strongly (positively) correlated with external forcings than are the AMOr timeseries. With volcanic forcing, the AMOnr correlations are significant for all models except BCC (mean correlations between 0.4 and 0.5 with all three volcanic forcing datasets~~. Similarly, the correlation~~), while with solar forcing the model

correlations are typically between ~~volcanic forcing and TAS are high (~~0.~~58 to~~ 0.~~79) for the CCSM4 and MPI. These strong~~ and 0.3. Removing the global-mean SST prior to calculating the AMO (i.e. AMOr) reduces the correlations with both volcanic and solar forcing (Fig. 8). The reconstructed WN17O series is not expected to correlate with external forcings because Wang et al. (2017) removed a regression estimate of the forced signal in reconstructed Atlantic SST to obtain this series. The other two reconstructions (WN17V and AMN09), however, also show only weak correlations with the external forcings.

Third, the simulated and reconstructed PDO timeseries do not correlate significantly with either volcanic or solar forcing (with a couple of exceptions that might be expected by chance – the IPSL model with volcanic forcing and the PMN09 reconstruction with SBF solar forcing). The means of the model correlations are close to zero.

These results explain some of the earlier findings concerning influences on E Asian temperature, specifically that external forcing strengthens its positive relationship with the AMO but weakens its (generally negative) relationship with PDO. Strong positive correlations demonstrate that natural external forcings ~~largely~~ cause concurrent warming or cooling in both the Atlantic and East Asian regions, contributing to the strengthening of positive correlations ~~found earlier~~ between ~~AMOnorem~~AMOnr and TAS in ~~these models~~the LMH simulations compared with the PI runs (Fig. ~~3g, h, i~~3 and 4). Removing the global SST anomaly first to obtain the ~~AMOrem~~AMOr index renders the correlations with volcanic forcing insignificant (Fig. 8) and the ~~AMOrem time series~~AMOr timeseries (Fig. ~~7d~~7e) do not show any cooling with corresponding volcanic forcing eruptions. This contributes to the much-reduced correlations with TAS when the ~~AMOrem~~AMOr series are used (Fig. 3 and 4).

~~The TAS-volcanic forcing relationship in the BCC model is notably weaker as is the AMO-volcanic forcing relationship (Fig.~~In terms of Pacific variability, the PDO is not strongly correlated with external forcing (as expected because it is diagnosed as an EOF of SST anomalies having first subtracted the global-mean SST). Therefore, adding external forcing does not greatly affect the PDO but it does cause additional variability in E Asian temperature, thus weakening the negative PDO-TAS relationship (Fig. 5 and 6; correlation measures the relative strength of their *common* variability). We might expect this effect to be particularly noticeable in those models that simulate a strong positive correlation between East Asian TAS and volcanic forcing (Fig. 8e). This is the case for CCSM4 (strong volcanic signal in TAS, adding the external forcing greatly weakens the PDO-TAS relationship) but not for MPI (strong volcanic signal in TAS but the PDO-TAS relationship is stronger in LMH than in PI, probably because this model has a negative PDO-volcanic correlation) nor BCC (the PDO-TAS relationship is weaker in LMH than in PI despite their being little influence of volcanic and solar forcings on E Asian temperature in this model).

~~8). This behaviour is the same if we use warm or cold-season TAS (not shown) rather than annual-mean TAS. The smaller influence of volcanic forcing for BCC partly explains why it has a weaker correlation between TAS and AMOnorem compared~~

~~to the CCSM4 and MPI models during the LMH simulations. The very weak BCC response to volcanic eruptions compared to CCSM4 and MPI models can be understood by comparing effective volcanic forcings in the three GCMs. To do this, we analyse net incoming shortwave radiation anomalies composited for the three largest volcanic eruption events (1257, 1458 and 1815) in all three models. Fig 9 shows that the decrease in the net incoming shortwave radiation following these eruptions in BCC is only ~20% of the response in both CCSM4 and MPI.~~

Since we can diagnose AMO and PDO timeseries that are not significantly correlated with volcanic forcing (Fig. 8: ~~AMOrem~~AMOr and the EOF-based PDO), we further tried factoring out the volcanic influence from the TAS time series to see if we could reproduce the behaviour of the control runs (~~PC) if we only had~~PI) using data from the forced runs (LMH). This is akin to trying to identify the behaviour of internal variability in the real Earth system (Steinman et al., 2015; Dai et al., 2015). We regressed volcanic forcing (~~GRA for BCC and CCSM4, and CEA for MPI here~~using the series for each model – Table 1) on the TAS data, and removed it to yield a TAS series without the linear influence of the volcanic forcing (~~See~~see section 2.4 ~~for detail~~). Factoring out volcanic forcing from TAS did weaken the correlations with the simulated AMO LMH series (Fig. 4; ~~AMOrem~~AMOnr vs ~~AMOrem~~AMOnr_vo~~) especially~~ for ~~CCSM4 and MPI. For example,~~ LMH) so that the mean of the model correlations ~~(Fig. 4)~~is very close to that found during the PI runs. However the TAS–AMOnr correlations for most individual models differ between ~~AMOnorem~~PI and the LMH with volcanic influenced factored out. Similar results are found using the AMOr index: there is agreement between PI and ~~TAS fall from 0.62–0.85 (AMOnorem) to 0.44–0.59 (AMOnorem_vo) and from 0.12–0.36 (AMOrem) to 0.12–0.23 (AMOrem_vo). The correlation didn't weak much for BCC (Fig. 4; AMOrem vs AMOrem_vo) because it simulates~~LMH correlations for the mean of the model correlations but not for the individual models (e.g. of the four models that show significant positive correlations in the PI runs, only ~~a weak~~two are significant in the LMH runs with volcanic influence on ~~E Asian temperature.~~TAS factored out). Despite factoring out the influence of the dominant forcing and using ~~a definition (AMOrem) that yields~~ an AMO index that is not strongly correlated with forcing, we still find very different behaviour in the ~~PC~~PI simulation than in the LMH simulation ~~for the MPI model: in the former, the role of AMO internal variability on E Asian temperature especially for the south part of E Asia is comparatively small than the latter.~~. For ~~the other~~ two models~~,~~ (BCC and CCSM4), we ~~can~~ correctly infer the small role of AMO internal variability on E Asian TAS from the LMH run ~~provided~~; for two models (MPI and CSIRO), we ~~factor out the influence of external forcings~~correctly infer a significant AMO role (though underestimating its importance for MPI); for two models (HadCM3 and IPSL) we fail to find the significant AMO role; and for MRI we find a significant AMO role despite its PI run showing no significant AMO role on E Asian TAS.

~~In terms of Pacific variability, the PDO is not strongly correlated with volcanic forcing: correlations are near zero for the BCC and CCSM4 models and slightly negative for MPI (Fig. 7e; Fig. 8). However, the CCSM4 and MPI models simulate strong positive correlations between East Asian TAS and volcanic forcing. This additional externally forced variability in East Asian~~

~~temperatures (due to the direct radiative cooling following strong volcanic eruptions) weakens the negative PDO-TAS correlation for BCC and CCSM4 (Fig. 6) but slightly strengthens it for MPI (likely because of the negative PDO-volcanic correlation).~~ Factoring out the volcanic signal ~~from TAS~~ hardly changes the ~~relationships~~simulated relationships between E Asian TAS and the PDO (~~LMH~~PDO_vo; Fig. 6). ~~This indicates that for two~~For some models ~~(BCC and CCSM4),~~, therefore, we are not able to determine the internal variability teleconnection between PDO and TAS ~~-~~when external forcings are present ~~even by~~despite using a PDO definition that is insensitive to external forcing and ~~by factoring~~regressing out the volcanic influence on TAS.

~~These results indicate that the surface temperature multidecadal variability over East Asia is strongly modulated by the external forcing rather than~~ This is especially for the two models (BCC and CCSM4) whose internal variability ~~in two of the models (Fig. 8). The percentages of variance (r^2) explained by the volcanic forcing are 62 % and 59 % for CCSM4 and MPI, respectively. This is in contrast to the WN18 TAS reconstruction, which~~ shows ~~no~~strong, significant ~~correlation with the volcanic series (WN18 also report that the volcanic signal is small compared with other influences). The PDO reconstructions show weakly negative (PMN09) or near zero (MD05) correlations with volcanic forcing, similar to the models. The AMO reconstructions by AMN09 and WN17V show positive correlation with the volcanic forcing time series, similar to the BCC model but much weaker than the other two models for the equivalent AMO index definitions (AMOnorem).~~associations between PDO and E Asian TAS but correlations are weak and insignificant in their LMH runs.

In the BCC model the relationship between volcanic forcing and both AMO and E Asian TAS is notably weaker than the other models (Fig. 8). This behaviour is the same if we use warm or cold-season TAS (not shown) rather than annual-mean TAS. ~~To further~~The smaller influence of volcanic forcing for BCC partly explains why it has the weakest correlation between TAS and AMOnr during the LMH simulations. To explore this weak BCC response to volcanic eruptions we analyse net incoming shortwave radiation anomalies composited for the three largest volcanic eruption events in all models (Fig. 9). This shows that the decrease in net incoming shortwave radiation following these eruptions in BCC is less than 25% of the response in both CCSM4 and MPI. The other four models lie between BCC and MPI. We also have analysed the same for the major volcanic events during the historical period for BCC, CCSM4 and MPI but did not find such a weak BCC response compared to the other two models. The weak volcanic forcing and response in BCC may be an artefact of how they implemented volcanic forcing in their last millennium simulation.

To assess the role of external forcing further, the power spectra of the AMO and PDO indices are analysed (Fig.10 and 11, respectively) ~~for the PC~~using the annual mean data (i.e. the data have not been low pass filtered before spectral estimation) for the PI and LMH experiments~~.~~, reconstructions and instrumental data. All ~~models display~~AMO timeseries have red spectra ~~with pronounced multidecadal variability~~(Fig. 10) at short timescales (up to 20 years) but ~~they differ in their peak frequencies. For~~

~~the AMOnorem method of diagnosing the AMO index~~at multidecadal timescales the redness, the absolute power and the presence of enhanced power across a broad range of frequencies all depend on the model, the presence/absence of forcing and the choice of AMO index. For the AMOnr index, the inclusion of external forcing (LMH runs) greatly strengthens the ~~redness and~~ multidecadal power of the variability ~~for the CCSM4 and MPI models~~; the increase is more moderate for BCC~~.~~ (see earlier discussion). Removing the global-mean SST first (~~AMOrem~~AMOr), reduces the difference between the ~~PC and LMH runs. The peak AMO frequency in BCC is about 20 years in most cases but there is a secondary peak around 60-80 years for AMOrem in the~~ PI and LMH ~~run. CCSM4 shows significant AMOrem spectral peaks at ~40 years (both PC and LMH) and also at ~20~~runs. Some models (BCC, HadCM3 and IPSL) show enhanced power at about 20 years, and there is prominent power around 30 years in the ~~LMH run. The MPI has the reddest AMO~~IPSL forced simulation (LMH) that is partly reduced using the AMOr index. In the reconstructions, the spectra ~~in all cases, with some runs/definitions showing peak power at ~~have steep gradients over the 40 to 60 year timescales, with elevated power above 60 years. In most models, variability around 60-80 years, often considered typical for the AMO, is quite strong but only for MPI is it notably elevated above the background red spectrum (CCSM4 has elevated power around 40-50 years. The AMO reconstructed spectra ~~allows us~~provide a comparison (Fig. 10a) ~~– not of the periodicity but~~ of the overall spectral shape. ~~CCSM4~~MPI, HadCM3 and ~~MPI~~IPSL models have the reddest spectra and for ~~AMOnorem~~AMOnr LMH these are qualitatively similar to the spectra of the WN17V and AMN09 reconstructions, while the ~~BCC model shows~~other models show much less multi-decadal power.

In the case of the PDO, all three models show red spectra with enhanced power at ~15-20 years for both ~~PC~~PI and LMH simulations, indicating that the Pacific variability arises mostly by internal variability. Landrum et al. (2013) found the same frequency for both control and last millennium simulations. The enhanced PDO power at ~15-20 years is filtered out by the 30-year smoothing used for the majority of analyses reported here, which might weaken the PDO-TAS correlation.

6. Discussion and Conclusions

The instrumental record is too short to clearly distinguish ~~the~~ contributions from natural internal variability, natural external forcings and anthropogenic forcings at multidecadal timescales. Zhang et al. (2018) and Wang et al. (2018) have explored this issue using paleoclimate reconstructions of temperatures over a large region in E Asia. Here, we complement these studies by using the dynamical information provided by three climate models (Table 1), with and without the influence of external forcings over the last millennium. Our key findings are:

1. The models simulate multidecadal modes of variability in the extratropical oceans (AMO and PDO) with spatial patterns similar to those previously identified in the observations and proxy-based reconstructions. Using commonly applied methods to diagnose their time series (area-averaged ~~N~~North Atlantic SST for the AMO and the leading EOF of ~~N~~North Pacific SST for the PDO) we find that they have red spectra with enhanced multi-decadal variability similar

to those found in observation and reconstructions. ~~The~~However, the shape and amplitude of their spectra ~~and the periods that have power significantly above the background spectrum~~ differ between the models and ~~with~~depend on the presence or absence of external forcing.

2. These multidecadal modes of variability, along with variations in volcanic forcing, are found to influence E Asian temperature in the models. In most cases, E Asia temperature is positively correlated with the AMO and volcanic forcing, and negatively correlated with the PDO. The correlations are not spatially uniform, with PDO correlations strongest in the parts of the E Asian region that are closest to the extratropical ~~N~~North Pacific Ocean, and the AMO influence showing some latitudinal ~~differences~~structure in most models.

3. The presence of external forcing strongly affects the apparent teleconnections between these multidecadal modes of variability and E Asia temperature. The effect depends on how the modes of variability are diagnosed and whether the forcings add common variability to both series (e.g., in the case of AMO) or add distinct variance to E Asia temperature but not to the mode of variability~~.~~ (e.g., in the case of PDO).

4. If the AMO is defined simply as the mean N Atlantic SST then external forcing strengthens the AMO-E Asia temperature correlation by causing concurrent warming or cooling in both the Atlantic and E Asian regions. For all ~~three~~seven models, the correlations between E Asian temperature and the AMO are stronger in the last millennium forced simulation than in their corresponding control runs when the AMO is defined this way.

5. Defining the AMO as the difference between N Atlantic and global-mean SST reduces ~~but does not completely remove this effect~~this effect but does not yield correlations between E Asian temperature and the AMO that match those present in the model control runs, because much but not all of the external forcing influence on N Atlantic SST also drives global SST in these models. ~~The AMO-E Asian temperature correlation is then much weaker in these models, and regressing~~ Despite factoring out the influence of the dominant forcing (volcanic) ~~from E Asian temperature further modifies this correlation~~on E Asian temperature and using an AMO index that is not strongly correlated with forcing, we still find different behaviour in the PI simulation than in the LMH simulation.

6. The PDO definition used here (the leading EOF of Pacific SST minus global-mean SST) yields an index that has only weak correlations with ~~volcanic~~external forcing. Despite this, the multidecadal correlation between the PDO and E Asia temperature (which is negative) is still sensitive to the presence of external forcing. In this case, external forcing weakens the apparent teleconnection in two of the models. This partly arises because external forcing (especially volcanic forcing) generates a response in E Asia temperature but not in the PDO index, thus weakening the correlation

between them. Regressing out the influence of volcanic forcing on E Asia temperature has ~~relatively~~ limited effect on the correlation, which remains much weaker than in the control run for two of the models.

These results have significant implications for attempts to determine the influence of the AMO and the PDO strictly as modes of *internal* variability on E Asia temperatures. With models, we can simply analyse their control runs. For the real world, we do not have that option: we can analyse only reconstructions from a real world in which natural external forcings are present. In this case, we recommend, on the basis of our results, that careful consideration be given to separating out the influence of external forcings on both the indices of modes of variability and on the E Asia temperature series before determining the internal variability teleconnections.

There are a number of ways to attempt this, each with ~~its own~~ limitations. The modes of variability might be defined using the difference between regional and global SST~~, however in many cases a separate~~. For example, the Last Millennium Reanalysis (Tardiff et al., 2019) provides globally-complete temperature fields that could be used (though these are not independent of the CCSM4 climate model or the forcings used). In many cases an independent reconstruction of global SST may not be available. Mann et al. (2009) reconstructed a global field of SST but prior to 1600 their reconstruction is a linear combination of only two spatial patterns which gives limited information about the Atlantic–global SST difference. Another approach is to identify and remove the influence of external forcing, e.g. by regression against forcing histories ~~-~~in reconstructions (Wang et al., 2017, 2018), by a method combining observations with ensemble of coupled climate model simulations (Dai et al., 2015 and Steinman et al., 2015), or using more sophisticated detection and attribution methods (e.g. Hegerl and Zwiers, 2011). These approaches require accurate forcing histories. A further approach is to use an EOF-based definition of the index where the spatial pattern has regions with loadings of opposite sign. External forcing tends to project similarly onto regions with opposite signs, cancelling out much of its influence on the resulting index. This is appropriate for the PDO, as used here, but less so for the AMO because the associated SST pattern is dominated by anomalies of the same sign (Fig. 1). Regression against forcing histories can also be used to remove the influence of external forcing on the target region (E Asian temperature for this study), prior to identifying the influence of AMO and PDO variability (Wang et al., 2018).

Even if these approaches are taken, it may still be impossible to determine the influence of multidecadal internal variability by analysing data that has been subject to external forcings. Despite factoring out the influence of the volcanic forcing in the AMO index, we still find ~~very~~ different behaviour in the forced simulation than in the control run for ~~the MPI model. In~~ some models. For example, in the forced run of the MPI model, the apparent AMO teleconnection on E Asian temperature is ~~rather weak (AMOrem~~only 0.4 (AMOr_vo in Fig. 4~~),~~) whereas in the control run it is strong~~.~~ (> 0.7 for AMOnr). For the ~~other two~~BCC and CCSM4 models, we can correctly infer from the forced run that ~~the~~ AMO internal variability has only a small influence on E Asia temperature ~~from the forced run~~ provided we ~~factor~~define the AMO as the difference between Atlantic

and global SST (just factoring out the influence of external forcings. from E Asia temperature in insufficient). Similar limitations were found regarding the PDO teleconnection: for two models (BCC and CCSM4), we are not able to determine its strongly negative correlation with E Asia temperature internal variability from a simulation with external forcings. We note the possibility that external forcing may have modified the dynamical behaviour of the internal variability in these cases, confounding the notion that we can clearly separate forced change from internal variability.

Finally, we found only partial agreement between the behaviours shown by the reconstructions and models. The correlations between E Asia temperature and the AMO and PDO showed the same signs in the models and the data, but the correlation values had a wide range. The strong influence of volcanic forcing in twosix of the models was not found in the reconstructions (Wang et al. 2018). We need to be careful while interpreting the results of the CMIP5-PMIP3 last millennium simulations in light of the paleoclimate record, because there exists a large uncertainties exist in the characterization of volcanic forcing, reconstruction of aerosol loading, optical depth and aerosol effective radius as a function of time, latitude, and height in the atmosphere, all of which exert important controls on the climate system (Atwood et al. 2016).

Acknowledgements.

Support provided by the Belmont Forum and JPI-Climate project INTEGRATE (An Integrated data-model study of interactions between tropical monsoons and extratropical climate variability and extremes) with funding by UK NERC grant NE/P006809/1. J.W. also acknowledges the support by the National Key R&D Program of China (grant: 2017YFA0603302) and the National Science Foundation of China (NSFC; grant: 41602192). We are thankful to two anonymous referees whose constructive comments helped to improve our study.

References

Ammann, C. M., Joos, F., Schimel, D., Otto-Bliesner, B., and Tomas, R.: Solar influence on climate during the past millennium: Results from transient simulations with the NCAR Climate System Model, Proc. Natl. Acad. Sci., 104, 3713, doi:10.1073/pnas.0605064103, 2007.

Atwood, A. R., Wu, E., Frierson, D. M. W., Battisti, D. S., and Sachs, J. P.: Quantifying climate forcings and feedbacks over the last millennium in the CMIP5-PMIP3, J. Climate, 29, 1161– 1178, 2016.

Bothe, O., Jungclaus, J. H., and Zanchettin, D.: Consistency of the multi-model CMIP5/PMIP3-past1000 ensemble, Clim. Past, 9, 2471–2487, doi:10.5194/cp-9-2471-2013, 2013.

Briffa, K. R., -Jones, P. D., Schweingruber, F. H., and Osborn, T. J.: Influence of volcanic eruptions on Northern Hemisphere summer temperature over the past 600 years. Nature, 393, 450–455, 1998.

Buckley, B. M., Ummenhofer, C. C., D'Arrigo, R. D., Hansen, K. G., Truong, L. H., Le, C. N., and Stahle, D. K.: Interdecadal Pacific Oscillation reconstructed from trans-Pacific tree rings: 1350–2004 CE. Climate Dynamics. https://doi.org/10.1007/s00382-019-04694-4, 2019.

Buntgen, U., Tegel, W., Nicolussi, K., McCormick, M., Frank, D., Trouet, V., Kaplan, J. O., Herzig, F., Heussner, K.-U., and Wanner, H.: 2500 years of European climate variability and human susceptibility, Science, 331, 578–582, 2011.

Christiansen, B., and Ljungqvist, F. C.: Challenges and perspectives for large-scale temperature reconstructions of the past two millennia. Reviews of Geophysics, 55, 40-96, 2017.

Coats, S., and Smerdon, J. E.: Climate variability: The Atlantic's internal drum beat. Nat. Geosci., 10, 470-471, 2017.

Coats, S., Smerdon, J. E., Cook, B. I., and Seager, R.: Stationarity of the tropical Pacific teleconnection to North America in CMIP5/PMIP3 model simulations. Geophys. Res. Lett., 40, 4927–4932, 2013.

Crowley, T. J., Zielinski, G., Vinther, B., Udisti, R., Kreutz, K., Cole-Dai, J., and Castellano, E.: Volcanism and the Little IceAge, PAGES Newslett., 16, 22–23, 2008.

Dai, A., Fyfe, J. C., Xie, S.-P., and Dai, X.: Decadal modulation of global surface temperature by internal climate variability. Nat. Clim. Change, 5, 555-559, 2015.

Delaygue, G. and Bard, E.: An Antarctic view of Beryllium-10 and solar activity for the past millennium, Clim. Dynam., 36, 2201–2218, doi:10.1007/s00382-010-0795-1, 2011.

Delworth, T. L., and Mann, M. E.: Observed and simulated multidecadal variability in the Northern Hemisphere. Climate Dyn., 16, 661–676, 2000.

Dufresne, J. L., Foujols, M. A., Denvil, S., Caubel, A., Marti, O., Aumont, O., Balkanski, Y., Bekki, S., Bellenger, H., Benshila, R., Bony, S., Bopp, L., Braconnot, P., Brockmann, P., Cadule, P., Cheruy, F., Codron, F., Cozic, A., Cugnet, D., de Noblet,

N., Duval, J. P., Ethe, C., Fairhead, L., Fichefet, T., Flavoni, S., Friedlingstein, P., Grandpeix, J. Y., Guez, L., Guilyardi, E., Hauglustaine, D., Hourdin, F., Idelkadi, A., Ghattas, J., Joussaume, S., Kageyama, M., Krinner, G., Labetoulle, S., Lahellec, A., Lefebvre, M. P., Lefevre, F., Levy, C., Li, Z. X., Lloyd, J., Lott, F., Madecm G., Mancip, M., Marchand, M., Masson, S., Meurdesoif, Y., Mignot, J., Musat, I., Parouty, S., Polcher, J., Rio, C., Schulz, M., Swingedouw, D., Szopa, S., Talandier, C., Terray, P., and Viovy, N.: Climate change projections using the IPSL-CM5 Earth System Model: from CMIP3 to CMIP5, Climate Dyn., 40, 2123–2165., 2013.

Fang, K., Cook, E., Guo, Z., Chen, D., Ou, T., Zhao, Y.: Syncronous multi-decadal climate variability of the whole Pacific areas revealed in tree rings since 1567.Environ. Res. Lett. 13 024016, ~~2018b~~2018.

Fang, K., Guo, Z., Chen, D., Wang, L., Dong, Z., Zhou, F., Zhao, Y., Li, J., Li, Y., Cao, X.: Interdecadal modulation of the Atlantic Multi-decadal Oscillation (AMO) on southwest China's temperature over the past 250 years. Clim Dyn., 52, 2055–2065, https://doi.org/10.1007/s00382-018-4244-x, ~~2018a~~2019.

Fleming, L. E., Anchukaitis, K. J.: North Pacific decadal variability in the CMIP5 last millennium simulations. Clim. Dyn., 47, 3783-3801, doi: 10.1007/s00382-016-3041-7, 2016.

Frank, D., Esper, J., Zorita, E., and Wilson, R.: A noodle, hockey stick, and spaghetti plate: a perspective on highresolution paleoclimatology, WIREs Climate Change, 1, 507–16, doi:10.1002/wcc.53, 2010.

Gao, C., Robock, A., and Ammann, C.: Volcanic forcing of climate over the past 1500 years: An improved ice core-based index for climate models. J. Geophys. Res., 113, D231111, doi:https://doi.org/10.1029/2008JD010239~~,~~, 2008.

Giorgetta, M. A., Jungclaus, J., Reick, C. H., Legutke, S., Bader, J., Böttinger, M., Brovkin, V., Crueger, T., Esch, M., Fieg, K., Glushak, K., Gayler, V., Haak, H., Hollweg, H.-D., Ilyina, T., Kinne, S., Kornblueh, L., Matei, D., Mauritsen, T., Mikolajewicz, U., Mueller, W., Notz, D., Pithan, F., Raddatz, T., Rast, S., Redler, R., Roeckner, E., Schmidt, H., Schnur, R., Segschneider, J., Six, K. D., Stockhause, M., Timmreck, C., Wegner, J., Widmann, H., Wieners, K.-H., Claussen, M., Marotzke, J., and Stevens, B.: Climate and carbon cycle changes from 1850 to 2100 in MPI-ESM simulations for the coupled model intercomparison project phase 5, J. Adv. Model. Earth Syst., 5, 572–597, doi:10.1002/jame.20038, 2013.

Hegerl, G., and Zwiers, F.: Use of models in detection and attribution of climate change. Wiley Interdiscip. Rev.: Climate Change, 2, 570–591, 2011.

Jones, P. D., and Mann, M. E.: Climate over past millennia. Rev. Geophys., 42:RG2002, doi:10.1029/2003RG000143, 2004.

Jones, P. D., Briffa, K. R., Osborn, T. J., Lough, J. M., van Ommen, T. D., Vinther, B. M., Luterbacher, J., Wahl, E. R., Zwiers, F. W., Mann, M. E., Schmidt, G. A., Ammann, C. M., Buckley, B. M., Cobb, K. M., Esper, J., Goosse, H., Graham, N., Jansen, E., Kiefer, T., Kull, C., Kuttel, M., Mosley-Thompson, E., Overpeck, ¨ J. T., Riedwyl, N., Schulz, M., Tudhope, A. W., Villalba, R., Wanner, H., Wolff, E., and Xoplaki, E.: High-resolution palaeoclimatology of the last millennium: a review of current status and future prospects, The Holocene, 19, 3–49, 2009.

Kerr, R. A.: A North Atlantic climate pacemaker for the centuries. Science, 288, 1984-1985, 2000.

Laepple, T., and P. H. Huybers, 2014: Ocean surface temperature variability: Large model–data differences at decadal and longer periods. Proc. Natl. Acad. Sci. USA, 111, 16 682–16 687, https://doi.org/10.1073/pnas.1412077111.

Landrum, L., Otto-Bliesner, B. L., Wahl, E. R., Conley, A., Lawrence, P. J., Rosenbloom, N., and Teng, H.: Last Millennium Climate and Its Variability in CCSM4, J. Climate, 26, 1085– 1111, doi:10.1175/JCLI-D-11-00326.1, 2013.

Li, X. et al. The East Asian summer monsoon variability over the last 145 years inferred from the Shihua Cave record, North China. Sci. Rep. 7, 7078, https://doi.org/10.1038/s41598-017-07251-3 (2017).

Li, X. L., Cheng, H., Tan, L. C., Ban, F. M., Sinha, A., Duan, W. H., Li, H. Y., Zhang, H. W., Ning, Y. F., Kathtayat, G., Edwards, R. L.: The East Asian summer monsoon variability over the last 145 years inferred from the Shihua Cave record, North China. Sci Rep 7:7078, 2017.

MacDonald, G. M., and Case, R. A.: Variations in the Pacific decadal oscillation over the past millennium. Geophys. Res. Lett., 32, L08703, doi:10.1029/2005GL022478, 2005.

Mann, M. E., Zhang, Z., Rutherford, S., Bradley, R. S., Hughes, M. K., Shindell, D., Ammann, C., Faluvegi, G., and Ni, F.: Global signatures and dynamical origins of the Little Ice Age and Medieval Climate Anomaly, Science, 326, 1256–1260, 2009.

Mann, M. E., and Lees, J. M.: Robust estimation of background noise and signal detection in climatic time series. Clim. Change, 33, 409-445, 1996.

Mantua, N. J., Hare, S. R., Zhang, Y., Wallace, J. M. and Francis, R. C.: A Pacific interdecadal climate oscillation with impacts on salmon production. Bull. Amer. Meteor. Soc., 78, 1069–1079, 1997.

Newman, M., and Coauthors, 2016: The Pacific Decadal Oscillation, Revisited. J. Clim., 29, 4399-4427.

Newman, M., Alexander, M. A., Ault, T. R., Cobb, K. M., Deser, C., Di Lorenzo, E., Mantua, N. J., Miller, A. J., Minobe, S., Nakamura, H., Schneider, N.: The Pacific decadal oscillation, revisited. J Clim. Doi: 10.1175/JCLI-D-15-0508.1, 2016.

Parsons, L. A., G. R. Loope, J. T. Overpeck, T. R. Ault, R. Stouffer, and J. E. Cole: Temperature and precipitation variance in CMIP5 simulations and paleoclimate records of the last millennium. J. Climate, 30, 8885–8912, https://doi.org/10.1175/JCLI-D-16-0863.1., 2017.

Phipps, S. J., Rotstayn, L. D., Gordon, H. B., Roberts, J. L., Hirst, A. C., and Budd, W. F.: The CSIRO Mk3L climate system model version 1.0—Part 1: Description and evaluation. Geosci. Model Dev., 4, 483–509, doi:10.5194/gmd-4-483-2011., 2011.

Phipps, S. J., Rotstayn, L. D., Gordon, H. B., Roberts, J. L., Hirst, A. C., and Budd, W. F.: The CSIRO Mk3L climate system model version 1.0—Part 2: Response to external forcings. Geosci. Model Dev., 5, 649–682, doi:10.5194/gmd-5-649-2012., 2012.

Qian, C. C., Yu, J.-Y., and Chen, G.: Decadal summer drought frequency in China: the increasing influence of the Atlantic Multi-decadal Oscillation. Environmental Research Letters, 9, 124004, 2014.

Rayner, N. A., Parker, D. E., Horton, E. B., Folland, C. K., Alexander, L. V., Rowell, D. P., Kent, E. C., and Kaplan, A.: Global analyses of sea surface temperature, sea ice, and night marine air temperature since the late nineteenth century. J. Geophys. Res., 108.4407, doi:10.1029/2002JD002670., 2003.

Schlesinger, M. E., and Ramankutty, N.: An oscillation in the global climate system of period 65–70 years. Nature, 367, 723–726., 1994.

Schmidt, G. A., Jungclaus, J. H., Ammann, C. M., Bard, E., Braconnot, P., Crowley, T. J., Delaygue, G., Joos, F., Krivova, N. A., Muscheler, R., Otto-Bliesner, B. L., Pongratz, J., Shindell, D. T., Solanki, S. K., Steinhilber, F., and Vieira, L. E. A.: Climate forcing reconstructions for use in PMIP simulations of the last millennium (v1.0), Geosci. Model Dev., 4, 33–45, doi:10.5194/gmd4-33-2011, 2011

Schmidt, G. A., Jungclaus, J. H., Ammann, C. M., Bard, E., Braconnot, P., Crowley, T. J., Delaygue, G., Joos, F., Krivova, N. A., Muscheler, R., Otto-Bliesner, B. L., Pongratz, J., Shindell, D. T., Solanki, S. K., Steinhilber, F., and Vieira, L. E. A.: Climate forcing reconstructions for use in PMIP simulations of the Last Millennium (v1.1), Geosci. Model Dev., 5, 185–191, doi:10.5194/gmd-5-185-2012, 2012.

Schurer, A. P., Hegerl, G. C., Mann, M. E., Tett, S. F. B., and Phipps, S. J.: Separating forced from chaotic climate variability over the past millennium. J. Clim., 26, 6954-6973, 2013.

Schurer, A. P., Tett, S. F. B., and Hegerl, G. C.: Small influence of solar variability on climate over the past millennium. Nat. Geosci., 7, 104-108, 2014.

Sigl, M., Winstrup, M., McConnell, J. R., Welten, K. C., Plunkett, G., Ludlow, F., Buntgen, U., Caffee, M., Chellman, N., Dahl-Jensen, D., Fischer, H., Kipfstuhl, S., Kostick, C., Maselli, O. J., Mekhaldi, F., Mulvaney, R., Muscheler, R., Pasteris, D. R., Pilcher, J. R., Salzer, M., Schupbach, S., Steffensen, J. P., Vinther, B. M., and Woodruff, T. E.: Timing and climate forcing of volcanic eruptions for the past 2,500 years, Nature, 523, 543–549, doi:10.1038/nature14565, 2015.

Smerdon, J. E. and Pollack, H. N.: Reconstructing Earth's surface temperature over the past 2000 years: the science behind the headlines, WIREs Clim. Change, 7, 746–771, https://doi.org/10.1002/wcc.418, 2016.

Smith, T. M., and Reynolds, R. W.: Improved extended reconstruction of SST (1854–1997). Journal of Climate 17: 2466–2477., 2004.

Steinhilber, F., Beer, J., and Fröhlich, C.: Total solar irradiance during the Holocene, Geophys. Res. Lett., 36, L19704, doi:10.1029/2009GL040142, 2009.

Steinman, B. A., Mann, M. E., and Miller, S. K.: Atlantic and Pacific multidecadal oscillations and Northern Hemisphere temperatures. Science, 347, 988-991, 2015.

Tardif, R., Hakim, G. J., Perkins, W. A., Horlick, K. A., Erb, M. P., Emile-Geay, J., Anderson, D. M., Steig, E. J., and Noone, D.: Last Millennium Reanalysis with an expanded proxy database and seasonal proxy modeling, Clim. Past, 15, 1251-1273, https://doi.org/10.5194/cp-15-1251-2019, 2019.

Taylor, K. E., Stouffer, R. J. and Meehl, G. A.: An overview of CMIP5 and the experiment design. Bull. Amer. Meteor. Soc., 93, 485–498, doi:https://doi.org/10.1175/BAMS-D-11-00094.1, 2012.

Trenberth, K. E., and Shea, D. J.: Atlantic hurricanes and natural variability in 2005. Geophys. Res. Lett., 33.L12704, doi:10.1029/2006GL026894, 2006.

Vieira, L. E. A., Solanki, S. K., Krivova, N. A., and Usoskin, I.: Evolution of the solar irradiance during the Holocene, Astron. Astroph., 531, A6, doi:10.1051/0004-6361/201015843, 2011.

~~Wang, J., Yang, B., Osborn, T. J., Ljungqvist, F. C., Zhang, H., and Luterbacher, J.: Causes of East Asiantemperature multidecadal variability during the last millennium. Geop. Res. Lett, Revised, 2018.~~

Wang, J., Yang, B., Ljungqvist, F. C., and Zhao, Y.: The relationship between the Atlantic Multidecadal Oscillation and temperature variability in China during the last millennium. J. Quat. Sci., 28, 653–658, doi:https://doi.org/10.1002/jqs.2658, 2013.

Wang, J., Yang, B., Ljungqvist, F. C., Luterbacher, J., Osborn, T. J., Briffa, K. R., and Zorita, E.: Internal and external forcing of multidecadal Atlantic climate variability over the past 1,200 years. Nat. Geosci, 10, 512–517, doi:https://doi.org/10.1038/ngeo2962, 2017.

Wang, J., Yang, B., Osborn, T. J., Ljungqvist, F. C., Zhang, H., and Luterbacher, J.: Causes of East Asian temperature multidecadal variability since 850 CE. Geophys. Res. Lett., 45,:13485-13494, doi:10.1029/2018GL080725, 2018.

Wang, Y.-M., Lean, J. L., and Sheeley Jr., N. R.: Modeling the Sun's Magnetic Field and Irradiance since 1713, Astrophys. J., 625, 522–538, doi:10.1086/429689, 2005

Xin, X. G., Wu, T. W., Li, J. L., Zhi, W. Z., Li, W. P., Wu, F. H.: How well does BCC CSM1.1 reproduce the 20th century climate change over China? Atmos Ocean Sci Lett., 6, 21–26, 2013.

Yukimoto, S., Adachi, Y., Hosaka, M., Sakami, T., Yoshimura, H., Hirabara, M., Tanaka, T.Y., Shindo, E., Tsujino, H., Deushi, M., Mizuta, R., Yabu, S., Obata, A., Nakano, H., Koshiro, T., Ose, T., Kitoh, A.: A new global climate model of the Meteorological Research Institute: MRI-CGCM3—Model description and basic performance, J. Meteorol. Soc. Jpn., 90a, 23–64., 2012.

Zhang, H., Werner, J. P. García-Bustamante, E., González-Rouco, F., Wagner, S., Zorita, E., Fraedrich, K., Ljungqvist, F. C., Zhu, X., Xoplaki, E., Chen, F., Duan, J., Ge, Q., Hao, Z., Ivanov, M., Schneider, L., Talento, S., Wang, J., Yang, B., and Luterbacher, J.: East Asian warm season temperature variations over the past two millennia, Scientific Reports, 8, 7702, 2018.

Table 1: Summary of the CMIP5-PMIP3 climate models considered in this study and the volcanic forcing applied in their Last Millennium simulations. The simulation length of last millennium and Historical simulations together for all the three models are 1151 years (850-2000). ~~The simulation length in the Pre-industrial control run for BCC, CCSM4 and MPI are 500 years, 1050 and 1150 years respectively.~~

			Resolution			Forcing	
Model (abbr.)	**Institution, Country**	**Reference**	**~~Atmospheric resolution~~Atmosphere**	**Ocean ~~resolution~~**	**~~Volcanic forcing~~ PI length (years)**	**Volcanic[1]**	**Solar[2]**
bcc-csm1-1 (BCC)	Beijing Climate Center, China	Xin et al. (2013)	128x64 L26	360x232 L40	~~Gao et al.~~ 500~~(2008)~~	GEA	VSK+ WLS
CCSM4 (CCSM4)	National Center for Atmospheric Research, USA	Landrum et al. (2013)	288x192 L26	320x384 L60	1050~~Gao et al. (2008)~~	GEA	VSK
MPI-ESM-P (MPI)	Max Planck Institute for Meteorology, Germany	Giorgetta et al. (2013)	196x98 L47	256x220 L40	1150~~Crowley et al. (2008)~~	CEA	VSK+ WLS
HadCM3 (HadCM3)	Met Office Hadley Centre, UK	Schurer et al. (2013)	96x73 L19	288x144 L20	1100	CEA	SBF+ WLS
MRI-CGCM3 (MRI)	Meteorological Research Institute, Japan	Yukimoto et al (2012)	320x160 L48	364x368 L51	500	GEA	DB+ WLS
IPSL-CM5A-LR (IPSL)	Institut Pierre Simon Laplace, France	Dufresne et al. (2013)	96x95 L39	182x149 L31	1000	GEA	VSK+ WLS
CSIRO Mk3L v1.2 (CSIRO)	University of New South Wales, Australia	Phipps et al. (2011, 2012)	64x56 L18	128x112 L21	1000	CEA	SBF

[1]**Volcanic forcings:** GAO = Gao et al. (2008); CEA = Crowley et al. (2008)

[1]**Solar forcings:** VSK = Vieira et al. (2011); DB = Delaygue and Bard (2011); SBF = Steinhilber et al. (2009); WLS = Wang et al (2005)

Table 2: Summary of the ~~paleo~~paleoclimate reconstructions considered in this study

Reconstruction (abbr.)	Reference	Variable	Time span	Data source
AMO (AMN09)	Mann et al. (2009)	N Atlantic average SST	500-2006	Tree ring, coral, ice & sediment cores
AMO (WN17V and WN17O)	Wang et al. (2017)	N Atlantic (0-70°N) average SST	800-2010	Tree ring, ice core, documentary
PDO (PMN09)	Mann et al. (2009)	N Pacific (22.5-57.5°N, 152.5°E-132.5°W) average SST	500-2006	Tree ring, coral, ice& sediment cores
PDO (MD05)	MacDonald & Case (2005)	N Pacific (north of 20°N) principal component of SST	993-1996	Tree ring
TAS (WN18)	Wang et al. (2018)	E Asia land air temperature	850-1999	Mean of 7 available reconstructions

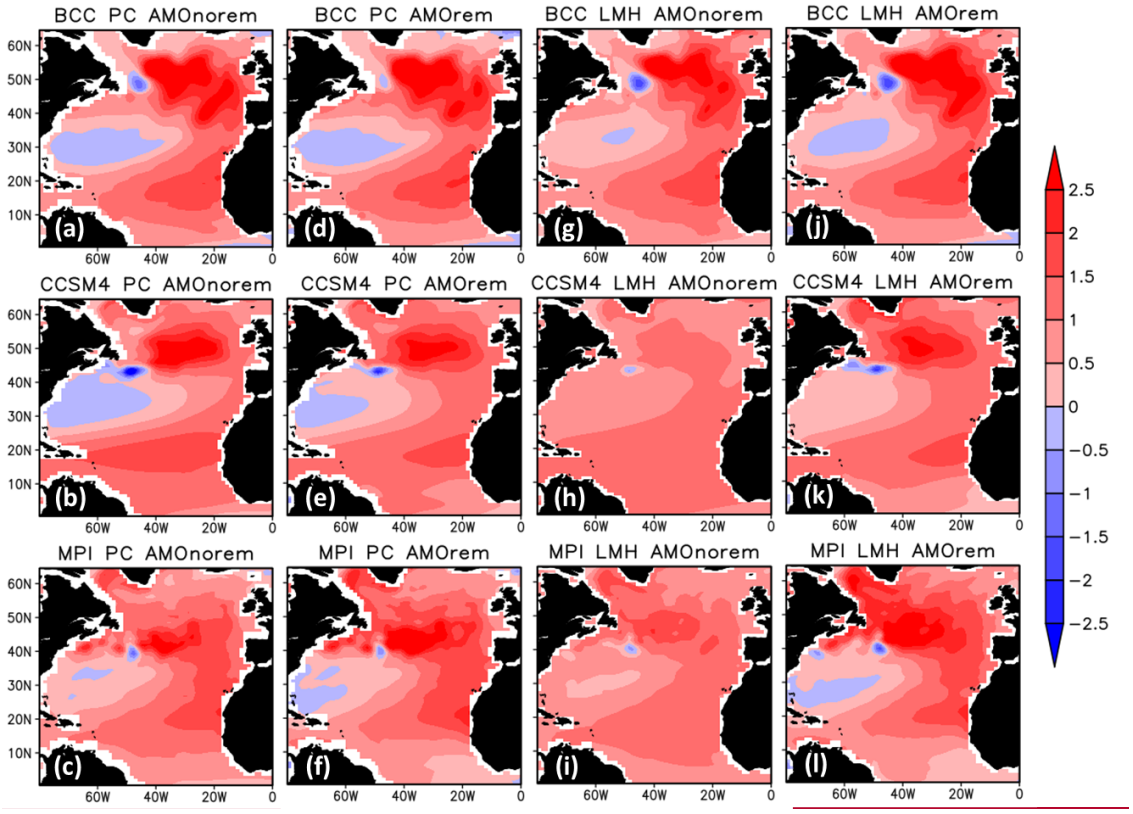
BCC PC AMOnorem
BCC PC AMOrem
BCC LMH AMOnorem
BCC LMH AMOrem
CCSM4 PC AMOnorem
CCSM4 PC AMOrem
CCSM4 LMH AMOnorem
CCSM4 LMH AMOrem
MPI PC AMOnorem
MPI PC AMOrem
MPI LMH AMOnorem
MPI LMH AMOrem
(a)
(b)
(c)
(d)
(e)
(f)
(g)
(h)
(i)
(j)
(k)
(l)
60N
50N
40N
30N
20N
10N
60W
40W
20W
0
2.5
2
1.5
1
0.5
0
−0.5
−1
−1.5
−2
−2.5

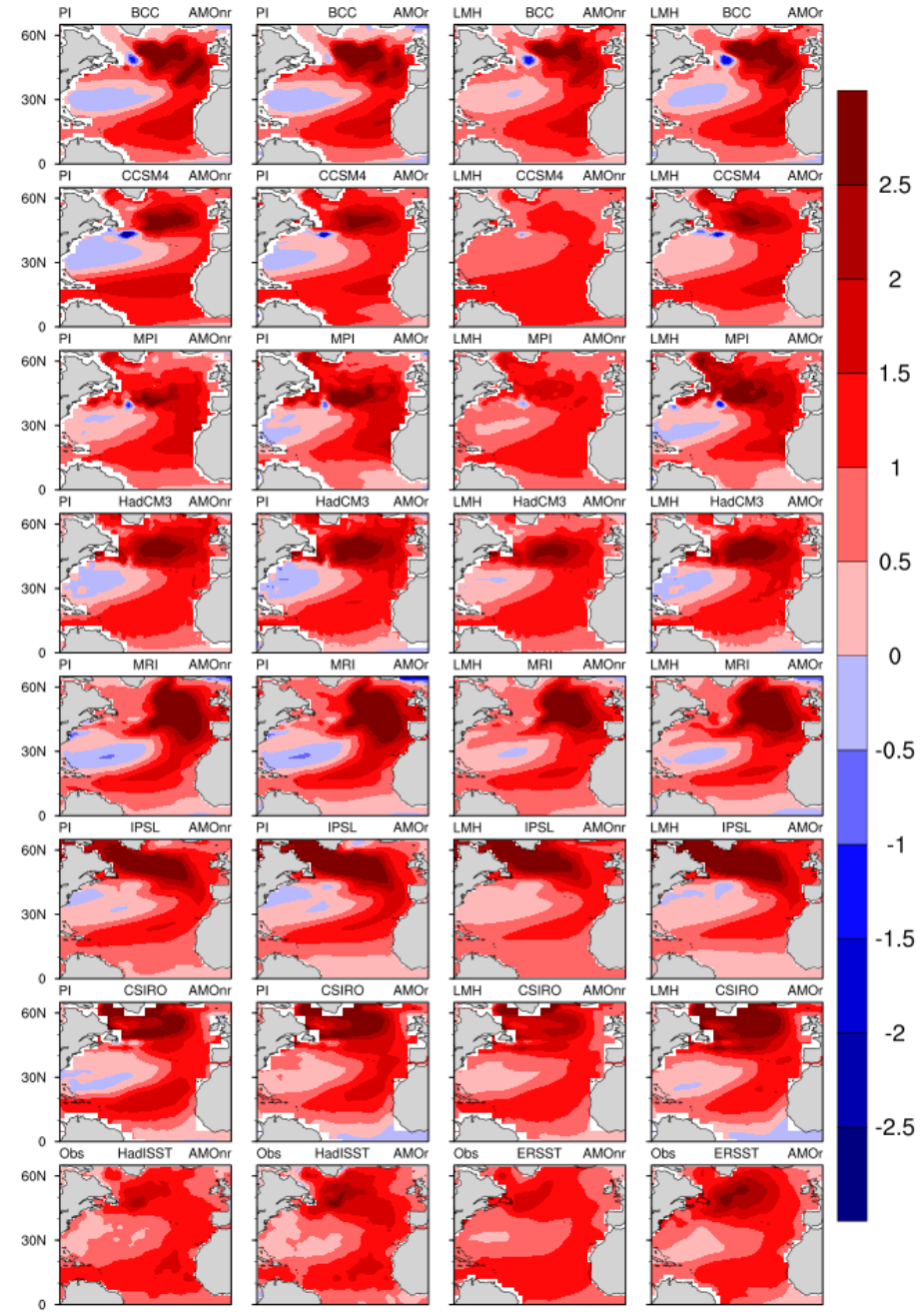

Figure 1: ~~The~~ AMO ~~spatial~~ patterns~~. Regression~~ defined by regression of annual mean SST on the AMO index for ~~the three CMIP models~~each GCM for the ~~LMH~~PI (1st and ~~PC~~2nd column) and LMH (3rd and 4th columns) experiments~~. (a, b, c) and (g, h, i)~~ compared with HadISST and ERSST observation (bottom row). 1st and 3rd columns use the AMO

index calculated without subtracting the global SST anomaly (AMOnr) while ~~(d, e, f)~~2nd and ~~(j, k, l)~~4th columns use the AMO index after subtracting the global SST anomaly~~.~~ (AMOr).

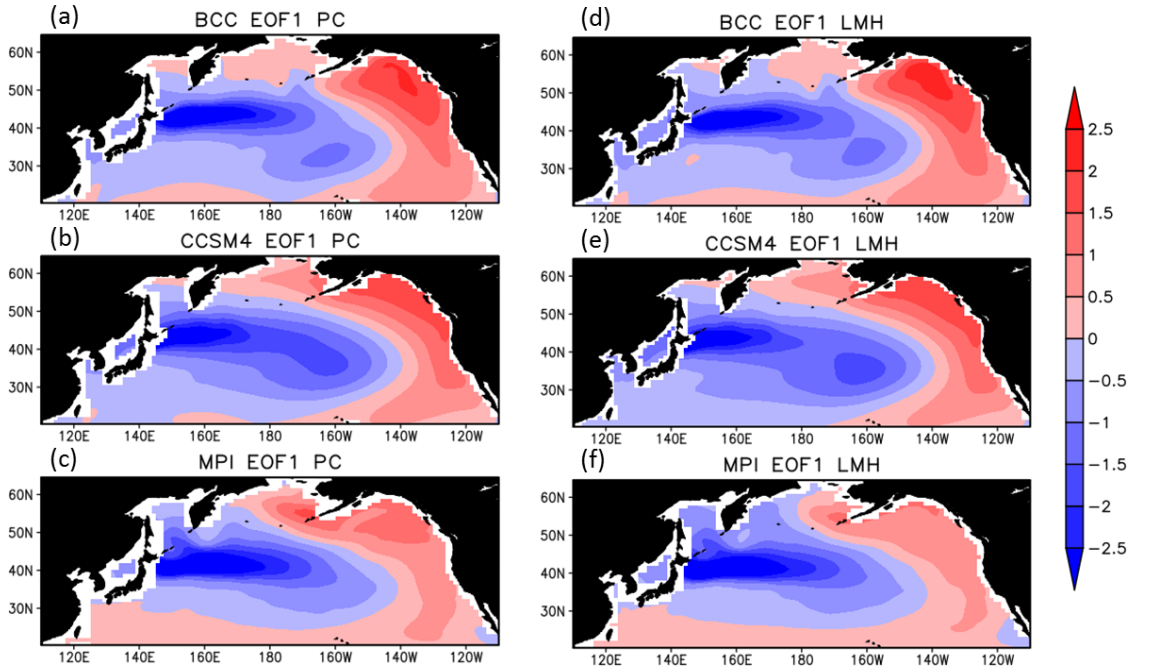
(a)
BCC EOF1 PC
(b)
CCSM4 EOF1 PC
(c)
MPI EOF1 PC
(d)
BCC EOF1 LMH
(e)
CCSM4 EOF1 LMH
(f)
MPI EOF1 LMH
60N
50N
40N
30N
120E
140E
160E
180
160W
140W
120W
2.5
2
1.5
1
0.5
0
−0.5
−1
−1.5
−2
−2.5

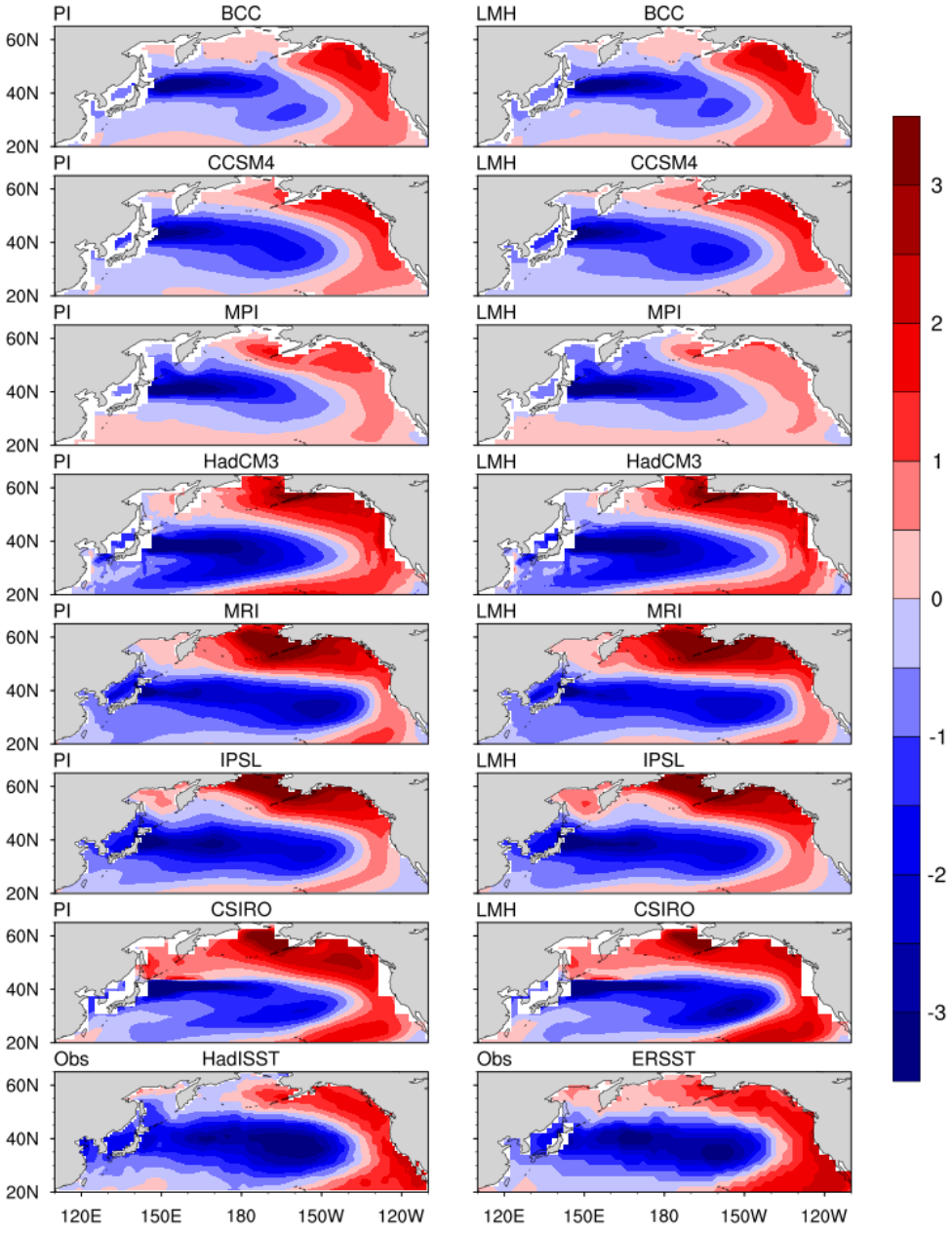

Figure 2: ~~The~~ **PDO** ~~spatial pattern. The leading~~SST patterns defined by the first **EOF of** ~~North Pacific~~annual mean **SST** ~~anomalies~~ **for** ~~the three CMIP models, PC (a, b, c~~each GCM for the PI (1st column) **and LMH (**~~d, e, f) simulations.~~2nd column) experiments compared with the HadISST and ERSST observations (bottom row).

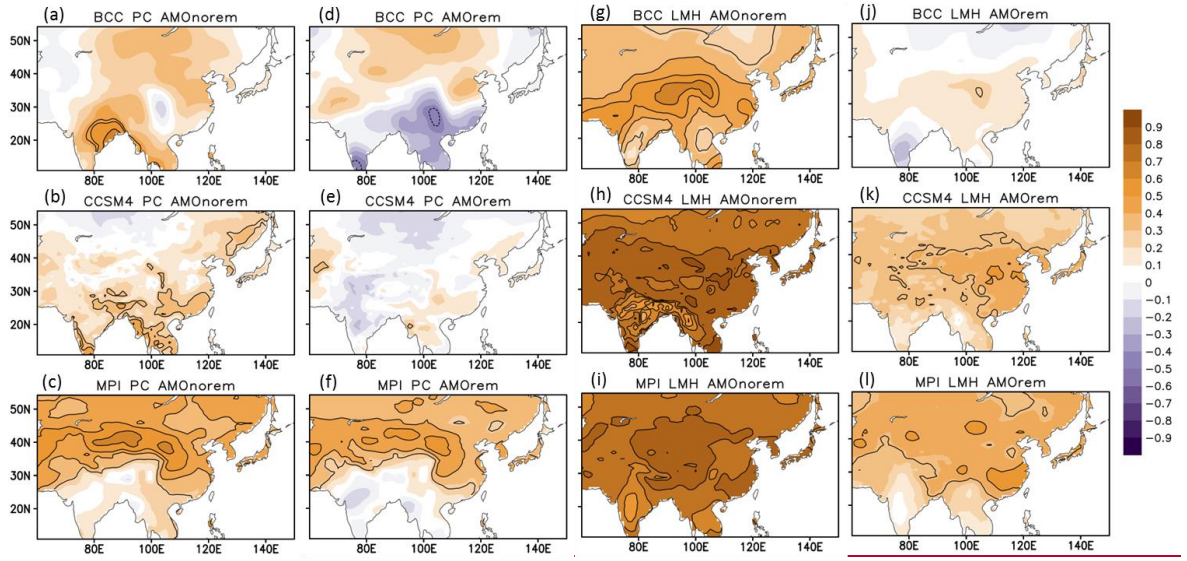
(a) BCC PC AMOnorem
(d) BCC PC AMOrem
(g) BCC LMH AMOnorem
(j) BCC LMH AMOrem
(b) CCSM4 PC AMOnorem
(e) CCSM4 PC AMOrem
(h) CCSM4 LMH AMOnorem
(k) CCSM4 LMH AMOrem
(c) MPI PC AMOnorem
(f) MPI PC AMOrem
(i) MPI LMH AMOnorem
(l) MPI LMH AMOrem
50N
40N
30N
20N
80E
100E
120E
140E
0.9
0.8
0.7
0.6
0.5
0.4
0.3
0.2
0.1
0
−0.1
−0.2
−0.3
−0.4
−0.5
−0.6
−0.7
−0.8
−0.9

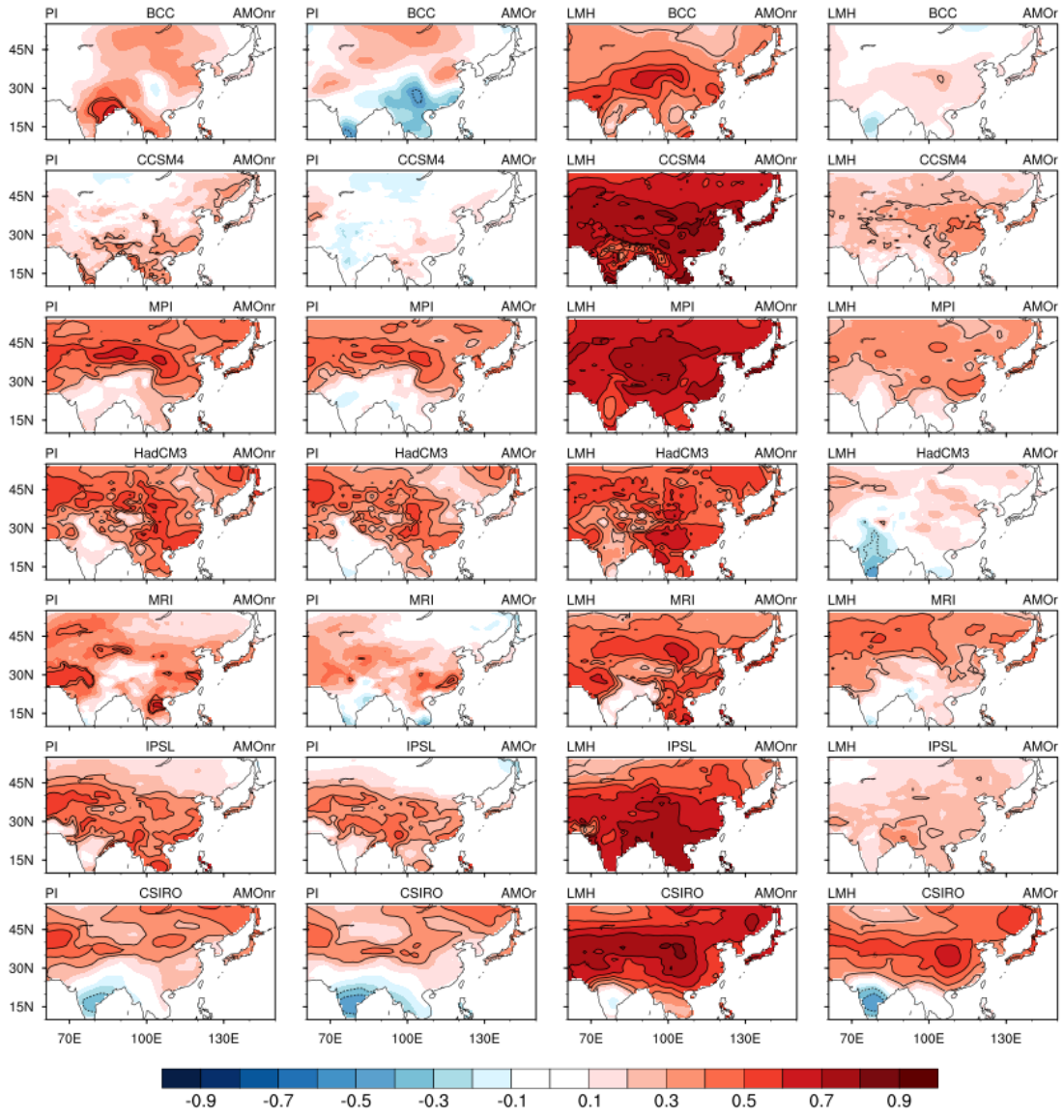

Figure 3: ~~The correlation~~Correlations between ~~AMO and~~annual mean East Asian surface ~~temperature at multidecadal timescales for the three CMIP models for the PC (a, b, c and d, e, f) and LMH (g, h, i and j, k, l) simulations. Correlations using the AMO index with (AMOrem, d, e, f~~temperatures and ~~j, k, l)~~AMO index for each GCM for PI (1st and ~~without (AMOnorem, a, b, c and g, h, i) subtracting global SST anomaly are also compared. The correlation~~2nd column) and LMH (3rd and 4th columns) experiments. AMOnr and AMOr are the two definitions of AMO index as described in Fig 1. Correlation values significant at 90% levels using two-tailed Student's t-test are contoured.

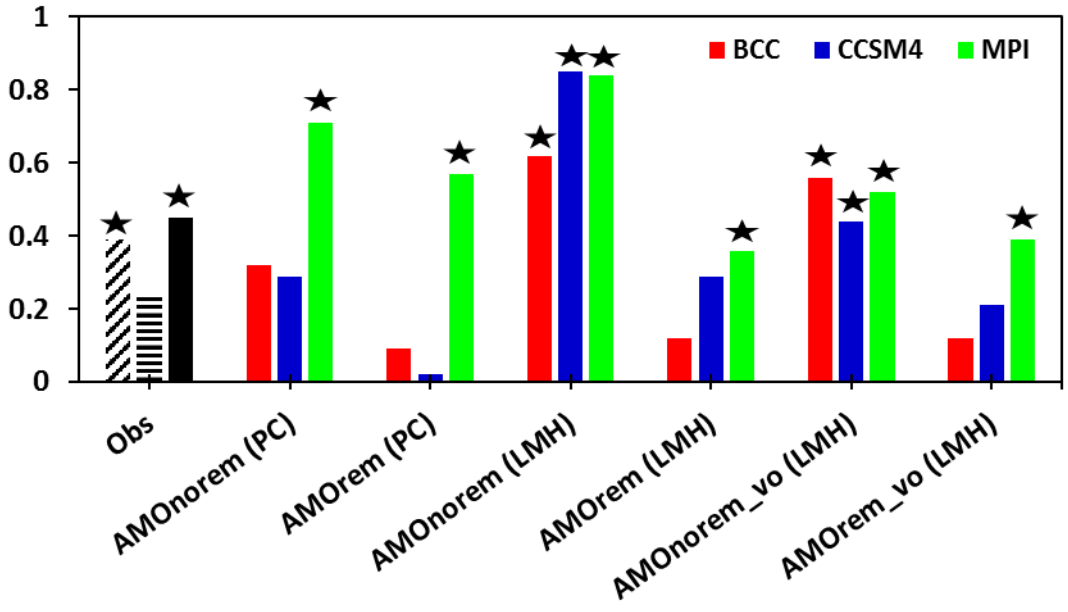
1
0.8
0.6
0.4
0.2
0
BCC
CCSM4
MPI
Obs
AMOnorem (PC)
AMOrem (PC)
AMOnorem (LMH)
AMOrem (LMH)
AMOnorem_vo (LMH)
AMOrem_vo (LMH)

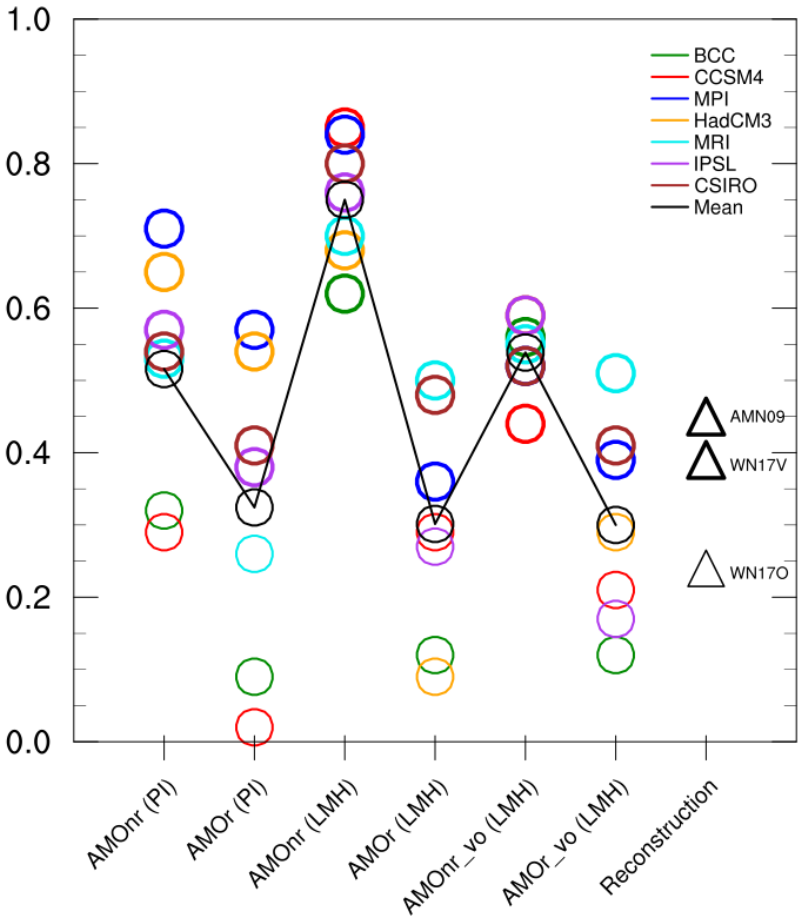

Figure 4: Correlations of ~~E~~annual mean East Asian regional average surface temperature against AMO for ~~models and also for the reconstructions (30-year low-pass filtered).The black dashed upward, dashed horizontal and solid bar are~~ each GCM (circles) for ~~observed correlation against TAS for WN17V, WN17O and AMN09 respectively. The groups of coloured bars are for different simulations (PC or LMH), different AMO definitions (global SST removed or not removed), and where~~ PI and LMH experiments compared with reconstructions (triangles). The mean correlations for the 7 GCMs are marked with black circles connected by a solid line. AMOnr and AMOr are the two definitions of AMO index described in Fig 1, while 'vo' indicates that the volcanic influence on ~~E~~East Asian temperature has been removed by linear regression ~~(vo).~~in the LMH experiments. The ~~bars marked with 'star' marks are significance~~thick circles and triangles show values significant at 95% level using a two-tailed student t-test. ~~The correlation for reconstructed~~The reconstruction correlations are between the WN18 E Asian temperature and the three AMO reconstructions (Table 2; the correlation with WN17O is weak (0.24) because it represents only internal AMO variability~~.~~

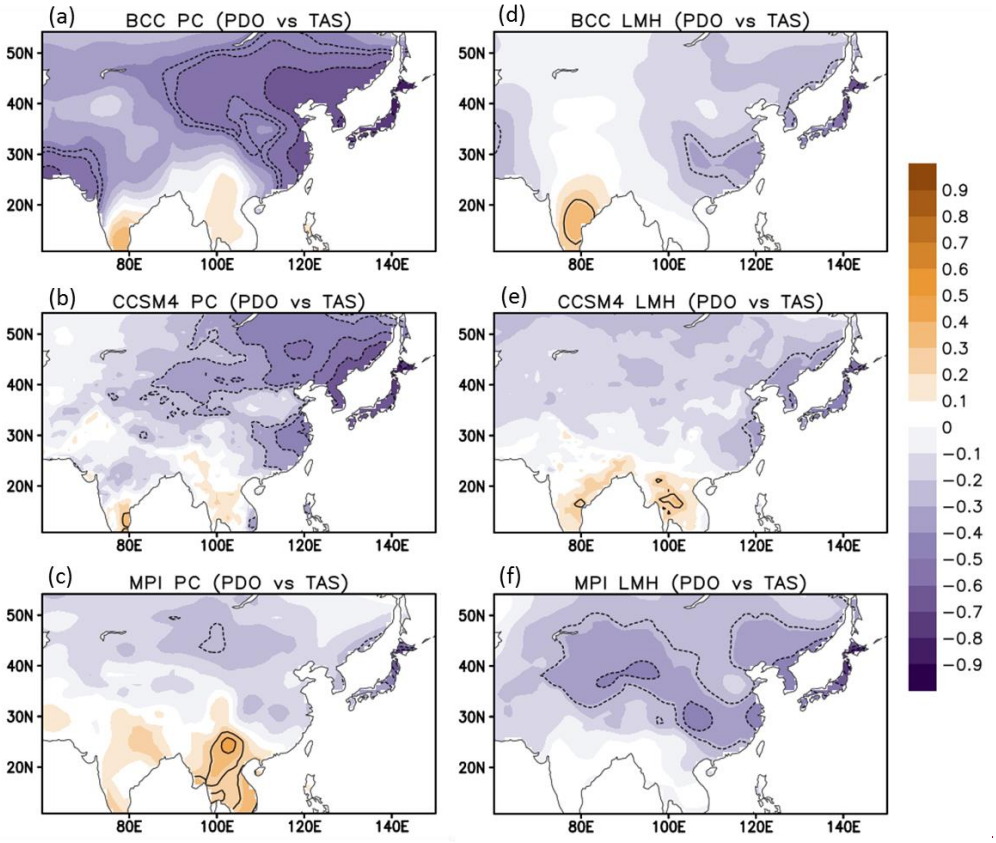
(a) BCC PC (PDO vs TAS)
(d) BCC LMH (PDO vs TAS)
(b) CCSM4 PC (PDO vs TAS)
(e) CCSM4 LMH (PDO vs TAS)
(c) MPI PC (PDO vs TAS)
(f) MPI LMH (PDO vs TAS)
50N
40N
30N
20N
80E
100E
120E
140E
0.9
0.8
0.7
0.6
0.5
0.4
0.3
0.2
0.1
0
−0.1
−0.2
−0.3
−0.4
−0.5
−0.6
−0.7
−0.8
−0.9

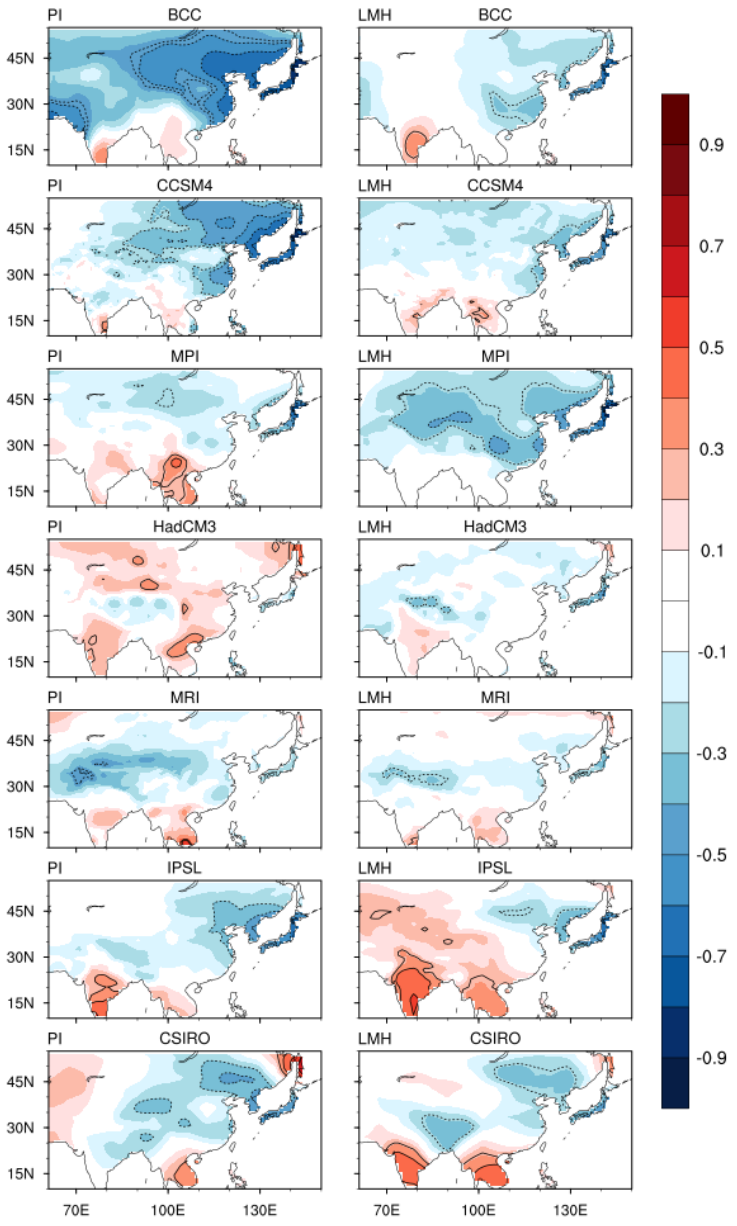

Figure 5: ~~The correlation~~Correlations between ~~PDO and~~annual mean East Asian surface ~~temperature at multidecadal timescales~~temperatures and PDO index for ~~the three CMIP models~~each GCM for ~~the PC (a, b, c~~PI (1st column) and LMH (~~d, e, f~~2nd column) experiments. ~~The correlation~~Correlation values significant at 90% levels using two-tailed Student's t-test are contoured.

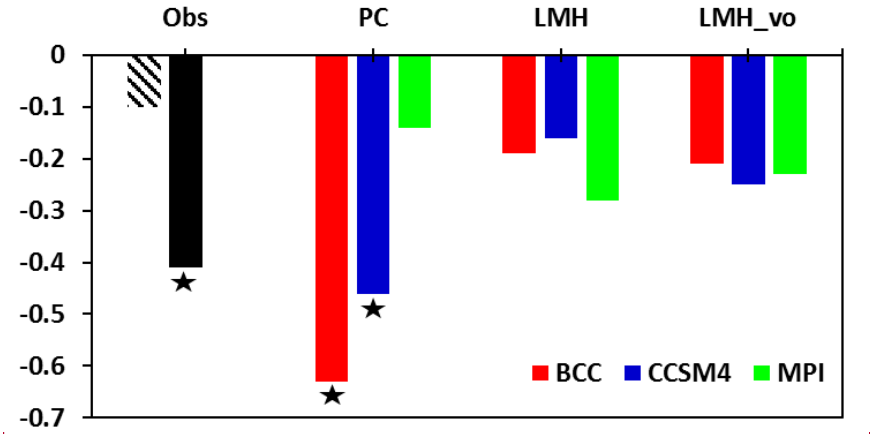
Obs
PC
LMH
LMH_vo
0
-0.1
-0.2
-0.3
-0.4
-0.5
-0.6
-0.7
BCC
CCSM4
MPI

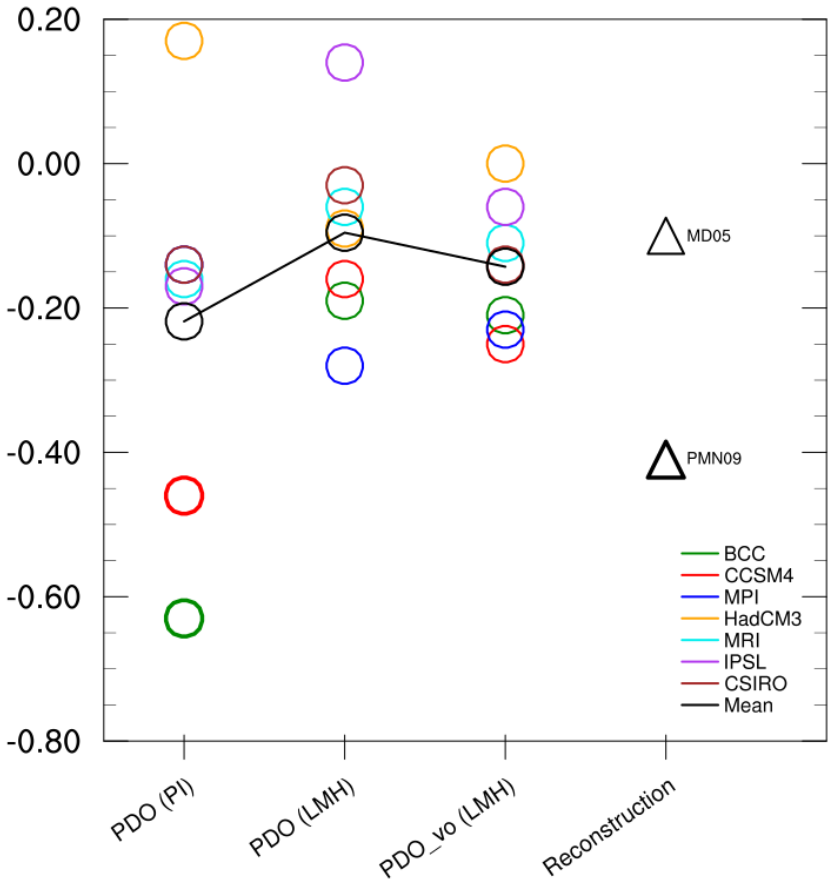
0.20
0.00
-0.20
-0.40
-0.60
-0.80
MD05
PMN09
BCC
CCSM4
MPI
HadCM3
MRI
IPSL
CSIRO
Mean
PDO (PI)
PDO (LMH)
PDO_vo (LMH)
Reconstruction

5

Figure 6: Correlations of ~~E~~annual mean East Asian regional average surface temperature against PDO ~~for models and also for the reconstructions (30-year low pass filtered). The black dashed and solid bar are for observed correlation against TAS for MD05 and PMN09 respectively. The bars marked with 'star' marks are significance at 95%~~ index for each GCM (circles) for PI and LMH experiments compared with reconstructions (triangles). The mean correlations for the 7 GCMs are marked with black circles connected by a solid line; 'vo' indicates that the volcanic influence on East Asian temperature has been removed by linear regression in the LMH experiments. The thick circles and triangles show values significant at 95% level using a two-tailed student t-test.

The reconstruction correlations are between the WN18 E Asian temperature and the two PDO reconstructions (Table 2).

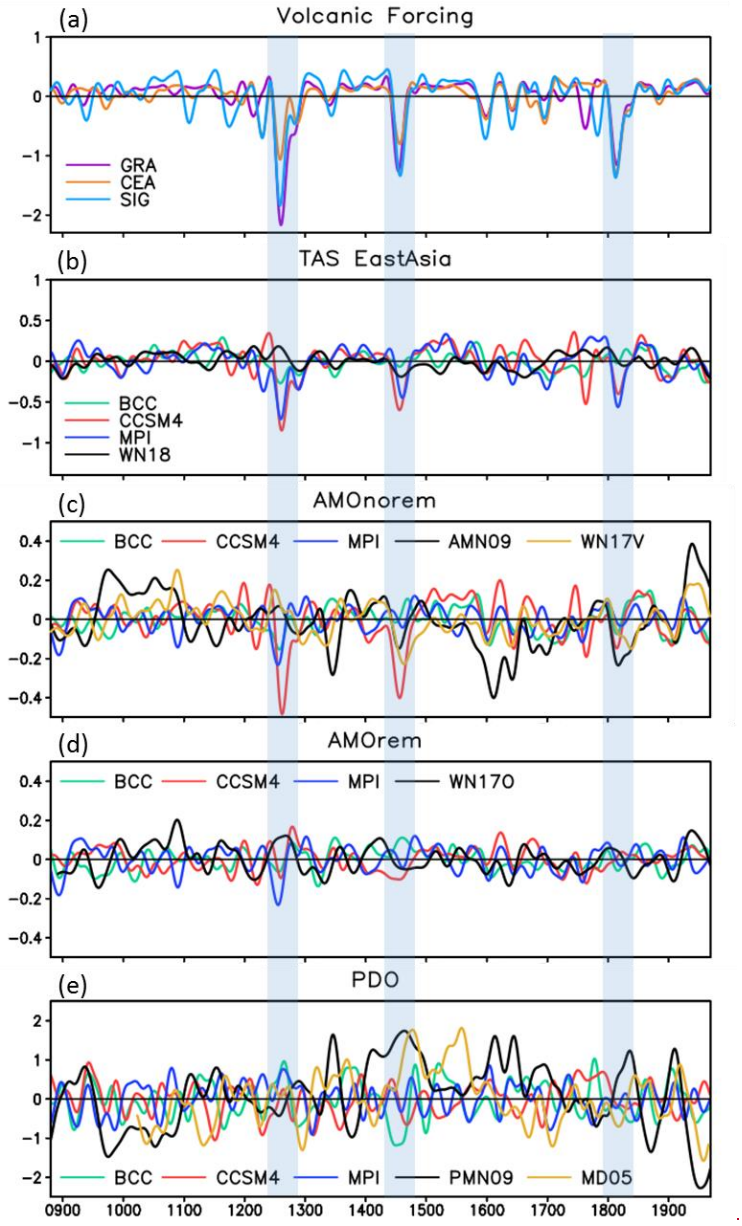

5

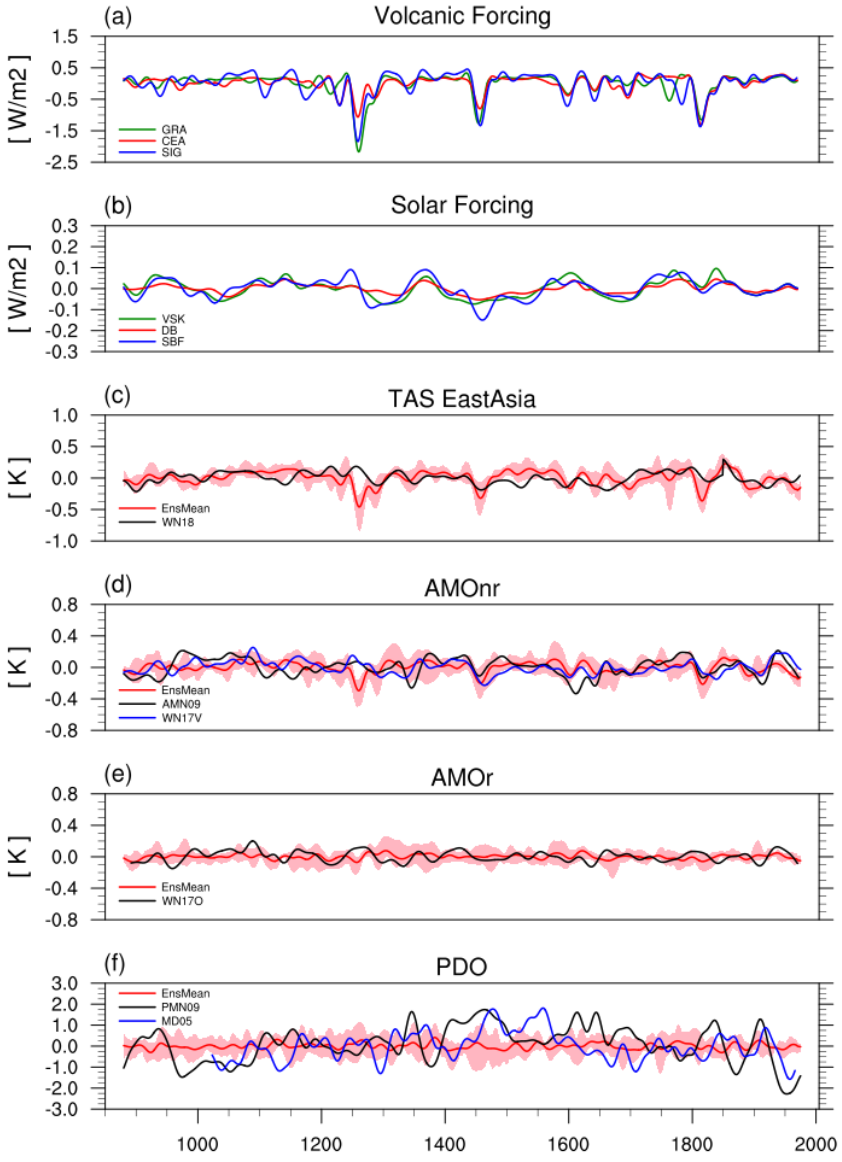

Figure 7: Timeseries of (a) volcanic forcing, (b) solar forcing, (c) surface temperature over East Asia, (~~c) AMO index without subtracting the global SST, (~~d) AMO index without subtracting the global SST (AMOnr), (e) AMO index after subtracting the global SST~~,~~ (AMOr), and (~~e~~f) PDO index, all are annual mean values, passed through a 30-year low pass filter and truncated to remove filter end effects. ~~Model simulation results are also~~Model simulations in (c)–(f) are given as the mean (red line) and spread (pink shading) of the 7 GCMs. Model simulations for surface temperature,

AMO and PDO are compared with the available reconstructed data. ~~MD05 PDO reconstructed data begins in 993, shorter than the other records. Blue vertical shading highlights the times when maxima of the filtered volcanic forcing occur.~~ (black and blue lines).

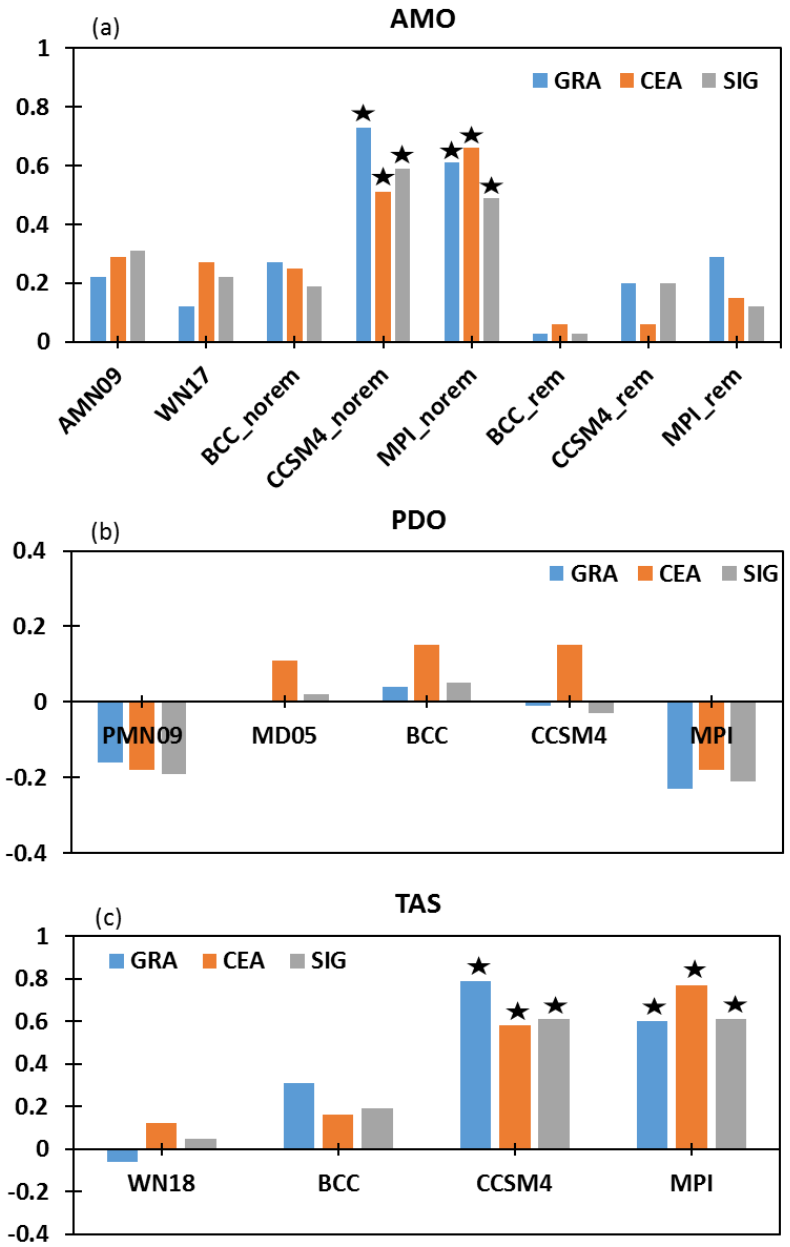

5

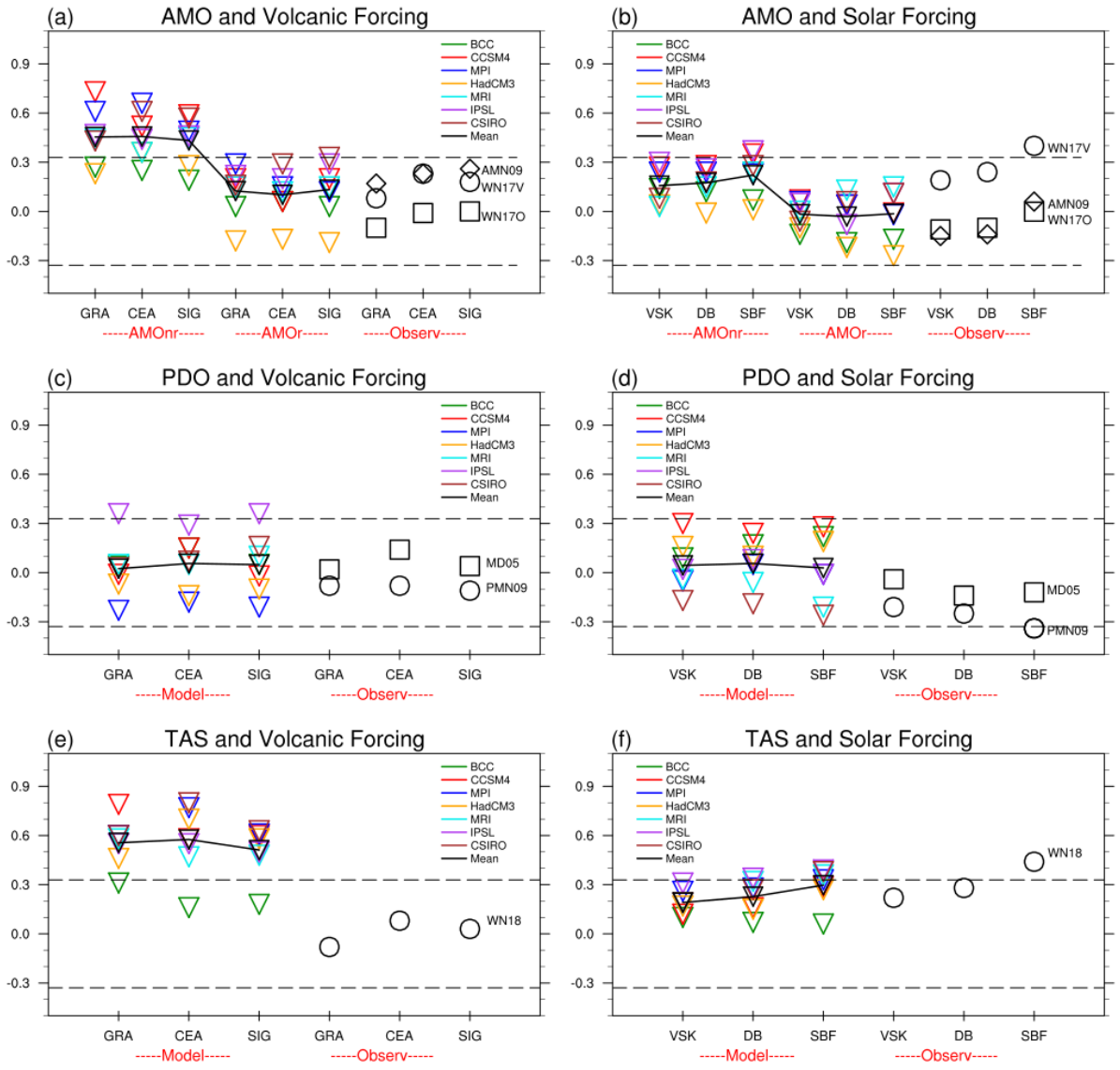

Figure 8: The correlations of ~~(a)~~annual mean AMO, ~~(b)~~ PDO and ~~(c)~~ TAS with volcanic forcing (~~models~~a, c, e) and ~~reconstructions)~~solar forcing (b, d, f) for each GCM (triangles) and reconstruction (circle, square and diamond). The threshold values for the individual correlations significant at 95% level using a two-tailed student t-test are marked as dashed lines. The means of the 7 model correlations are shown by black triangles connected by black lines.

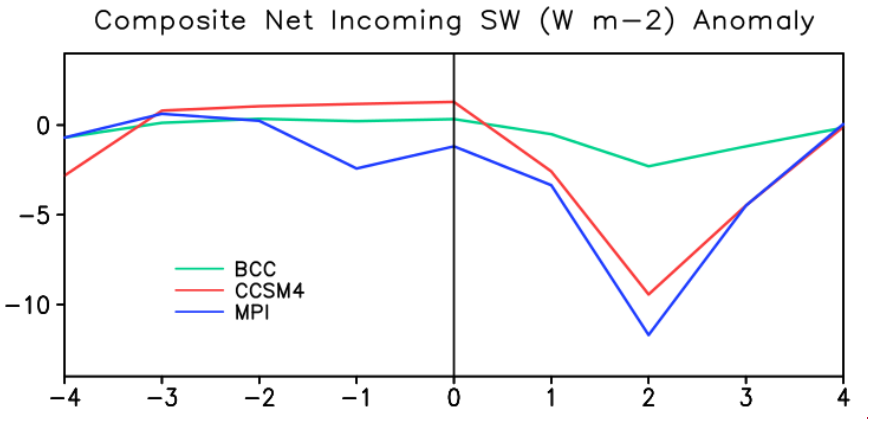
Composite Net Incoming SW (W m−2) Anomaly
0
−5
−10
BCC
CCSM4
MPI
−4
−3
−2
−1
0
1
2
3
4

5

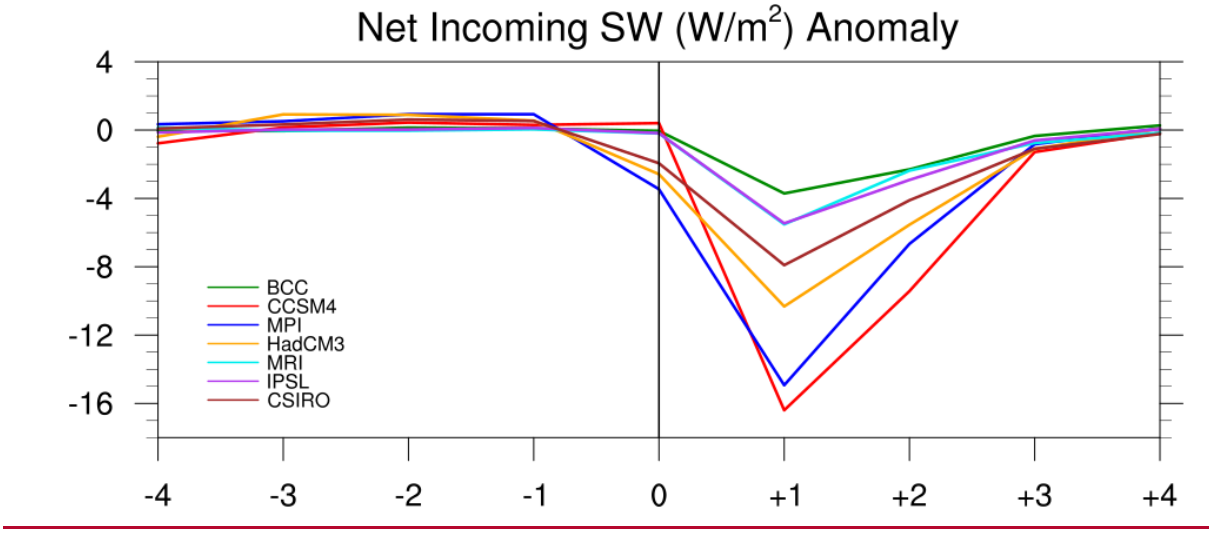

Figure 9: Annual mean composite anomaly of net shortwave (SW) radiation at the top of the atmosphere for three large volcanic eruption events ~~(1257, 1458 and~~for each GCM. Individual GCM results are aligned so that their peak negative SW anomalies occur at year+1 (i.e. 1258, 1452, 1815~~). The zero vertical line is the year volcanic eruptions occurred and the numbers left and right of it are the years before and after the event.~~ for BCC, CCSM4, IPSL; 1258, 1452, 1816 for MRI; 1258, 1456, 1816 for MPI, HadCM3, CSIRO).

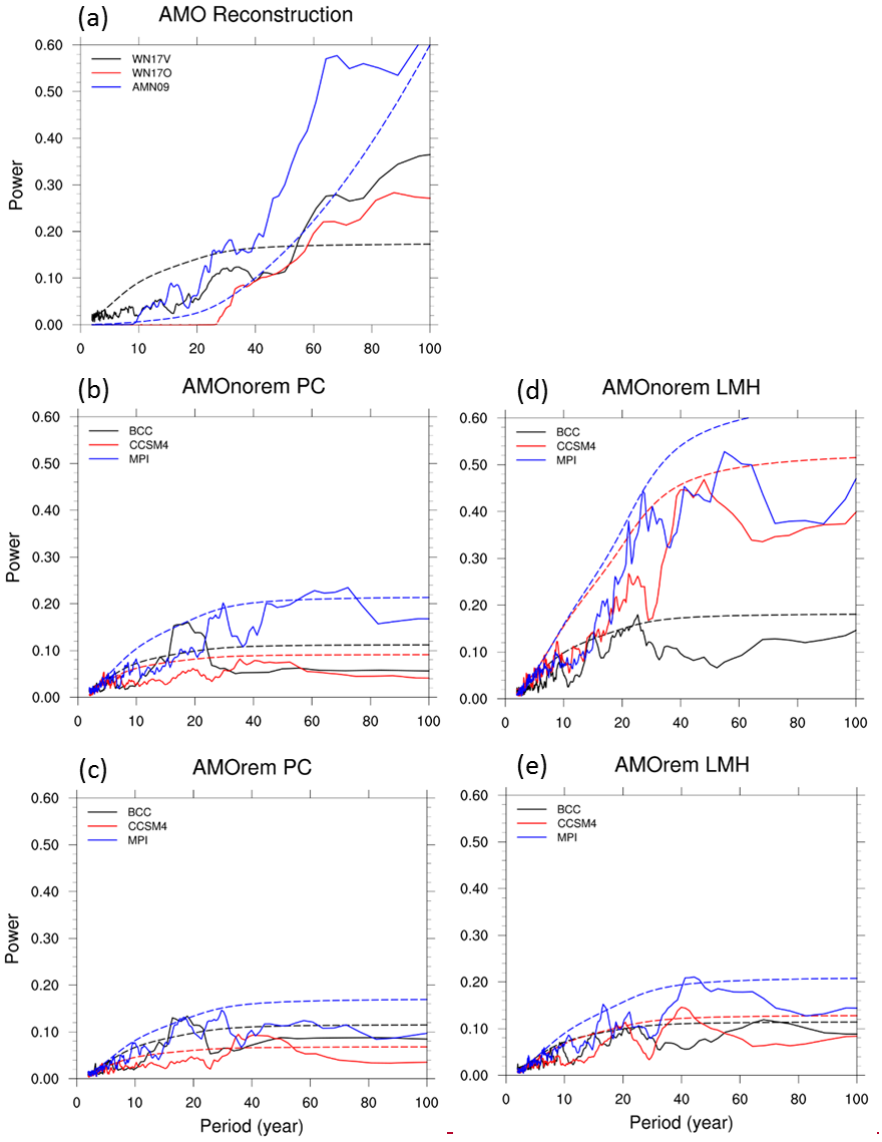
(a) AMO Reconstruction
WN17V
WN17O
AMN09
Power
(b) AMOnorem PC
(d) AMOnorem LMH
(c) AMOrem PC
(e) AMOrem LMH
BCC
CCSM4
MPI
Period (year)

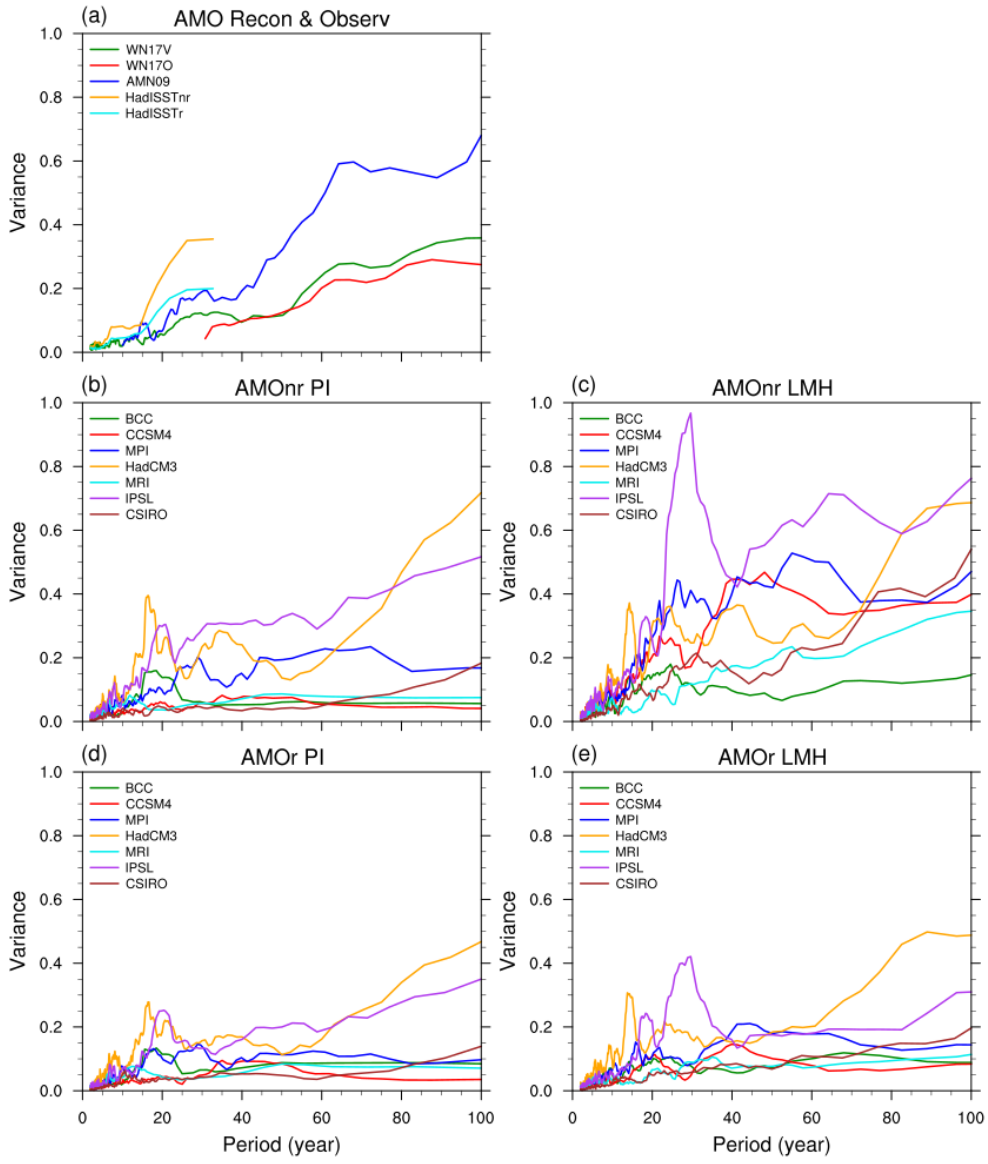

Figure 10: **Spectra of AMO index of reconstructions and instrumental data (a) and ~~three models~~each of 7 GCMs for ~~PC~~PI (b and ~~c~~d) and LMH (~~d~~c and e) experiments. AMOnr and ~~also~~AMOr are the two definitions of AMO index ~~with (c and e) and without (b and d) first subtracting the global SST anomaly. The solid lines are spectra and dashed lines~~ described in Fig 1. Spectra are ~~confidence at 90% level of periods with significantly higher variability than expected from an autoregressive spectrum. For WN17O (solid red line),~~not shown for timescales that the ~~power for periods~~ underlying data cannot adequately represent (not for < 30 years ~~is zero and should be ignored~~for WN17O and not for**

< 10 years for AMN09 because ~~only~~these reconstructions use 30-year and 10-year low-pass filtered data ~~were available and hence~~ respectively; not for > 30 years for HadISST because the ~~dashed line for confidence level is not presented (a). instrumental data is too short to determine power on longer timescales).~~

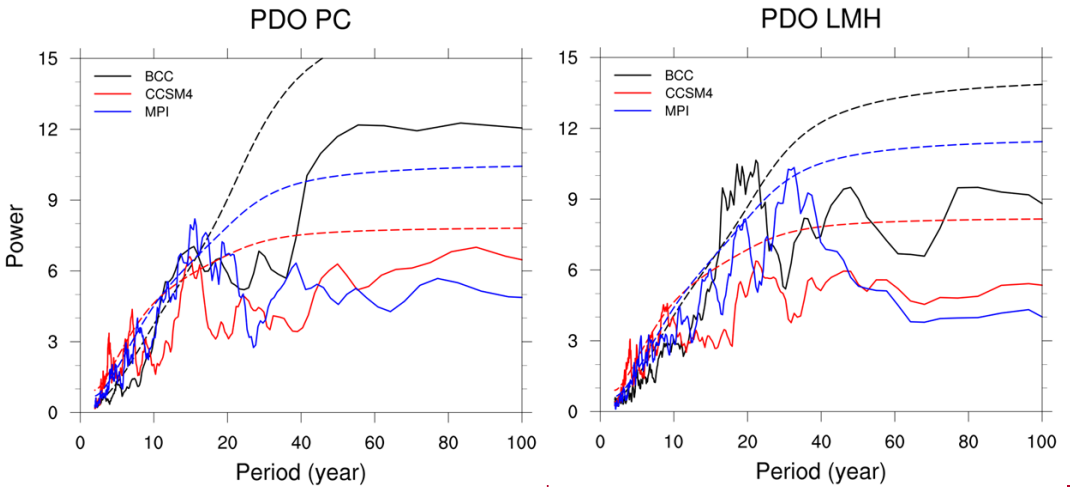
PDO PC
PDO LMH
BCC
CCSM4
MPI
Power
Period (year)
0
3
6
9
12
15
0
10
20
40
60
80
100

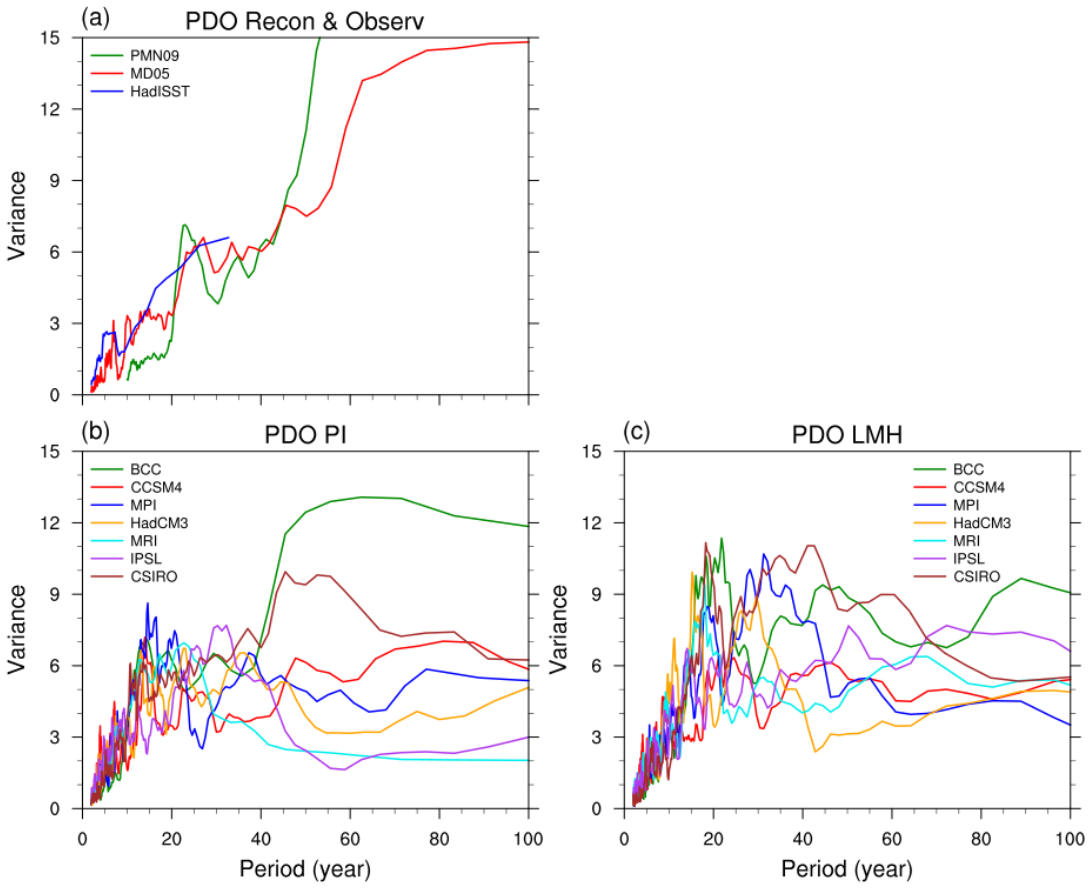

Figure 11: Spectra of PDO index of ~~three models~~ reconstructions and instrumental data (a) and GCMs for ~~PC~~PI (b) and LMH (c) experiments. ~~The solid lines~~Spectra are ~~spectra and dashed lines are confidence at 90% level of periods with significantly higher variability than expected from an autoregressive spectrum.~~not shown for timescales that the underlying data cannot adequately represent (not for < 10 years for PMN09 because this reconstruction uses 10-year low-pass filtered data; not for > 30 years for HadISST because the instrumental data is too short to determine power on longer timescales).